
UV NEWS

The official newsletter of the Thematic Network for Ultraviolet Measurements



Issue 10 / July 2014



Contents

Editorial	3
EMRP ENV03 Traceability for surface spectral solar ultraviolet radiation	4
Development of an array spectroradiometer with improved stray light rejection using band-pass filters	4
Improvements to the μ -MUV Spectroradiometer prototype for reduced stray-light	6
Characterisation of nonlinearities of array spectroradiometers in use for measurements of the terrestrial solar UV irradiance	9
Application of a dual-channel solid state spectrometer to measure spectral radiation and atmospheric constituents	12
Multi-spectral UV sky camera: MUSKY	17
Using a laser driven light source for spectral responsivity calibration of detectors between 250 and 400 nm wavelengths	20
A Laser-Driven Light Source (LDLS) as a portable spectral irradiance calibration source in the UV range	22
Improved diffusers for spectroradiometers measuring solar irradiance	25
Devices for characterizing the wavelength scale of UV spectrometers	28
Regular articles	30
The GUVis-3511: a new multi-channel radiometer for monitoring UV and visible radiation	30
Characterization of UV photodiodes in the ultraviolet spectral region	31
The J1006 total sky camera for fast and accurate cloud detection	34
News	35
NIWA UV Workshop	35

ISSN 1456-2537

Unigrafia, Espoo 2014

UVNews is the official newsletter of the Thematic Network for Ultraviolet Measurements. The Network was originally funded by the Standards, Measurements and Testing programme of the Commission of the European Communities, as project number SMT4-CT97-7510. During 2011 – 2014 the Network receives financing from the Euramet through project EMRP ENV03 “Traceability for surface spectral solar ultraviolet radiation” and in 2014 – 2017, through project EMRP ENV59 “Traceability for atmospheric total column ozone.” *UVNews* is published at irregular intervals. It is aimed to exchange knowledge between the participants of the Network and to disseminate information on the forthcoming and past activities of the Network. The newsletter also contains scientific and technical articles on UV measurements and a news-section about activities in the field of UV measurements. The newsletter welcomes all announcements and articles that might be of importance for the readers. The editor of the Newsletter may be reached by:

Aalto University
Metrology Research Institute
Petri Kärhä
P. O. Box 13000
FI-00076 Aalto, Finland

<http://metrology.hut.fi/uvnet/>

E-mail: petri.karha@aalto.fi

In case of all material to publish, submission by E-mail is preferred. The next issue will be published in March 2016.

*Photographs: Cover: Devices participating in the UV intercomparison in Davos in July 2014 (Picture by Tomi Pulli).
Page 3: Participants of the UVNet workshop in Davos on July 15 – 16, 2014 (Picture by PMOD).*

Editorial

Petri Kärhä

Aalto University, Espoo, Finland

One part of the history of the Thematic Network for Ultraviolet Measurements is coming to a successful end. The EMRP project ENV03 “Traceability for surface spectral solar ultraviolet radiation” has reached its final destination at the end of July 2014. Luckily this does not end our activities – the Network will receive further funding from a continuation project ENV59 “Traceability for atmospheric total column ozone.” With this funding, we can continue for three more years, publish two new issues of *UVNews*, and arrange training activities.

The Solar UV project ENV03 was a success with many measures. Many new techniques for improved solar measurements were developed and tested. This Issue of *UVNews* presents some of them, including diffusers with improved cosine response, array spectroradiometers improved in various ways with e.g. a micro-mirror chip, band-pass filters and mathematics, and a novel sky camera taking 2π photographs of the sky at various UV wavelengths. Various characterisation setups were developed as well. Linearity of array spectrographs can now be reliably measured at various institutes. Laser driven light sources have been tested for calibration purposes. Wavelength calibrations can be improved with new “rulers.”

Project ENV03 culminated in a UV Workshop and a solar UV intercomparison at Davos in July 2014. Various instruments participated in the intercomparison, where it was possible to see all new instruments developed, to characterise and calibrate own instruments, and of course to compare. The weather during the intercomparison week was not particularly good, but luckily the

proceeding workshop week was sunny, so the measurements continued another week.

UVNews 11 will be published around February 2016. By that time, the new project EMRP ENV59 ATMOZ will have almost reached its mid-point. The progress of the project will thus be reviewed. This newsletter will be collected by the end of 2015. To receive the call for articles, please register to the *UVNet* mailing list (<http://metrology.tkk.fi/uvnet/lists.htm>) if you do not receive our E-mails already. The same page can be used to unsubscribe from the mailing list.

Finally, I would like to wish you all a nice end of summer and beginning autumn and hope to see you in the coming UV activities!



EMRP ENV03 Traceability for surface spectral solar ultraviolet radiation

Development of an array spectroradiometer with improved stray light rejection using band-pass filters

J. Dubard and T. Valin

Laboratoire national de métrologie et d'essais, Trappes, France

Introduction

Solar UV irradiance measurements in the 280 – 400 nm spectral range require specific measurement conditions because of the rapidly varying Sun irradiance level on the 10 s time scale. Array spectroradiometer is potentially a good instrument that can meet these requirements. However these spectroradiometers suffer from stray light that can lead to large error in the short wavelength UVB range (280 – 300 nm) of the Sun spectral irradiance. Stray light can be characterized with the spectral line-spread function method (SLF) using a tunable laser, and a correction of the measured spectrum can be performed by applying for instance the Zong method [1], to get the true spectrum. Even though improvement of measurement can be achieved using this method, the

uncertainty is still large because of the uncertainty on the SLF characterization. Therefore, a reduction of the stray light contribution is necessary to improve the solar UV irradiance measurement uncertainty. In the framework of the ENV03 project task 4.4, we propose to use band-pass filters to reduce the spectral bandwidth of the incoming light inside the spectroradiometer and hence reduce the stray light contribution.

We present first the characteristics of the spectroradiometer and the characterizations performed: transmission of the filters, linearity, temperature behaviour, stray light (SLF), spectral calibration, noise level, measurement stability. Then performances of the modified spectroradiometer are given.

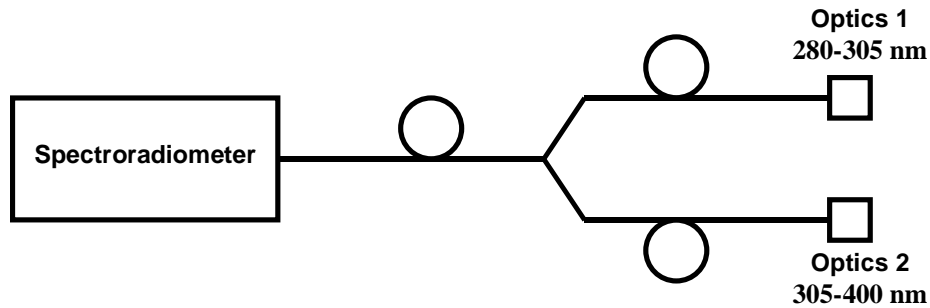


Figure 1. Schematic of the modified spectroradiometer.

Spectrometer development

The modified spectroradiometer is based on a Jobin Yvon VS140 array spectroradiometer. The measurement spectral range is 200 – 650 nm. However, the spectroradiometer is optimized for UV operation by choosing the CCD chip, the UV imaging grating, and by properly aligning the optical elements to insure a spectral bandwidth of about 1 nm over the 280 – 400 nm spectral range.

Measurement of Sun spectral irradiance is challenging due to the five to six orders of magnitude difference in irradiance between 280 nm and 400 nm wavelengths. The critical part is the 280 – 300 nm range for which stray light contributes significantly to the measured signal. To achieve reduction of the stray light, particularly below 300 nm, and still have substantial signal to noise ratio, it is necessary to have at least two filter sets. Therefore, the operating principle of the modified spectroradiometer is shown in Fig. 1.

The spectroradiometer is fitted with a 600 μm diameter 1x2 optical fiber in order to overfill the 35 μm wide, 500 μm height of the entrance slit of the spectrometer. The two input fibers are connected to two cosine response diffuser heads equipped with dedicated filters. The cosine response diffusers have been developed elsewhere in the project [2]. The first head is equipped with an interference filter, with central wavelength of 290 nm and a spectral bandwidth of 30 nm, and a 3 mm thick UG11 type filter, and is operated on the 280 – 305 nm spectral range. The spectral transmittance of this filter combination is shown in Fig. 2 (violet line). The second head is equipped with a 0.5 mm thick UG11 type filter, and is operated in the 305 – 400 nm spectral range. The heads are equipped with mechanical shutters in order to allow alternative measurement in the two spectral ranges. The spectroradiometer is installed in a thermal box at 20 °C to minimize thermal effects on the wavelength scale and CCD responsivity.

Characterization of the spectroradiometer

The spectroradiometer is characterized for the following parameters: wavelength scale accuracy, signal linearity, thermal behaviour, stray light. The wavelength accuracy is within ± 0.1 nm and no wavelength shift is noticed when varying the ambient temperature from 0 °C to 40 °C. The linearity of the CCD chip is good over the 60000 counts signal level (16 bits ADC). Stray light is characterized at PTB with the TULIP laser facility. The SLF characteristics of the 280 – 305 nm head are shown in Fig. 3. Similar behaviour is seen for the 305 – 400 nm head showing a low stray light contribution. Peaks on the right side of the graph are due to second order diffraction and have no effect on the measured signal. No leakage of the out of band light is noticeable.

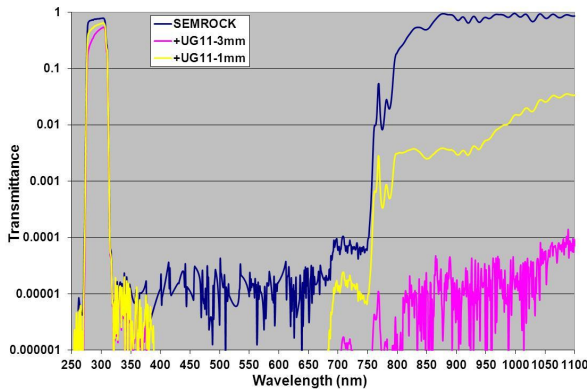


Figure 2. Spectral transmittance of different filter combinations for the 280 – 305 nm head.

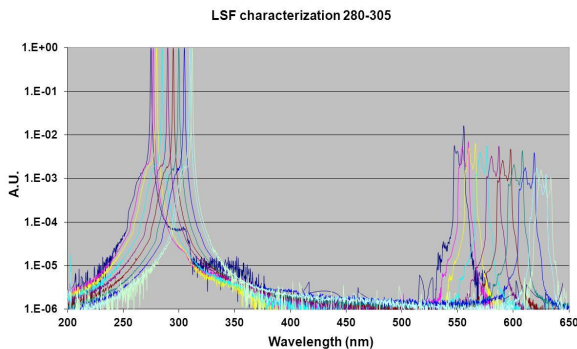


Figure 3. Spectral line-spread function of the spectroradiometer.

Performance

The spectroradiometer took part in the comparison that was held in July 2014 at PMOD in Davos. A typical Sun irradiance measurement with the new device is shown in Fig. 4. The data are not corrected for stray light and the measurement time is about 15 s.

The data indicate that the spectroradiometer exhibits four orders of magnitude measurement capabilities on the 300

– 400 nm spectral range [3]. Comparison to Quasume reference spectroradiometer has shown good agreement within ± 2 %. On the 300 – 310 nm spectral range which is the overlapping region of the two heads, no increased noise has been noticed on the spectra measured throughout the day indicating that temperature effects on the transmission of the filters placed inside the heads is not an issue. For wavelength < 300 , nm deviation from the reference spectroradiometer should be corrected taking into account the stray light.

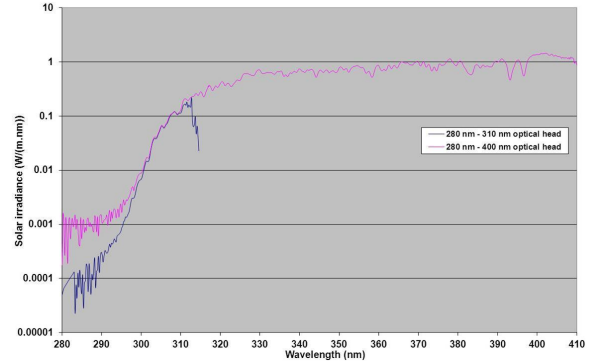


Figure 4. Sun spectral irradiance measurement.

Conclusions

We have developed an array spectroradiometer with reduced stray light contribution by use of band-pass filters to perform Sun spectral irradiance measurement on the 280 – 400 nm spectral range. This instrument allows measurements on four orders of magnitude dynamic range without additional stray light correction and on a time scale of about 10 s. This is a cost effective solution for fast and accurate spectral measurements in UV applications.

Acknowledgement This work has been supported by the European Metrology Research Programme (EMRP) within the joint research project ENV03 “Traceability for surface spectral solar ultraviolet radiation” (SolarUV). The EMRP is jointly funded by the EMRP participating countries within EURAMET and the European Union.

References

- [1] Y. Zong, S.B. Brown, B.C. Johnson, K.R. Lykke, and Y. Ohno, “Simple spectral stray light correction method for array spectroradiometers,” *Appl. Opt.* **45**, 1111–1119 (2006).
- [2] P. Kärhä, J. Mes, T. Pulli, J. Schreder, A. Partosobroto, G. Huelsen, J. Askola, and J. Gröbner, “Improved diffusers for spectroradiometers measuring solar irradiance,” *UVNews* **10**, 25–27 (2014).
- [2] L. Egli et al., “New technologies to reduce stray light for measuring solar UV with array spectroradiometers,” *IRS2012 Proceedings*, Berlin (2012).

Improvements to the μ -MUV Spectroradiometer prototype for reduced stray-light

Ari Feldman^{1,2}, Geiland Porovecchio², Marek Smid², and Kathryn Niel³

1. National Institute of Standards and Technology, Boulder, CO, USA
2. Cesky Metrologicky Institut, Prague, Czech Republic
3. Measurement Standards Laboratory of New Zealand, Callaghan Innovation, Lower Hutt, New Zealand

The ultraviolet (UV) solar spectrum below 320 nm is difficult to measure because it contains 6 orders of magnitude of dynamic range [1]. Traditional double scanning monochromators are able to effectively measure the spectrum with little stray-light contribution, yet when considering the changing spectrum of solar radiation, the long scanning acquisition time is not appropriate. Faster acquisition methods such as diode-array spectroradiometers provide a low-cost alternative which are capable of capturing the spectrum within seconds. However, due to the nature of the compact optics and single chamber layout, the signal in the UV range below 320 nm is dominated by stray-light contributions from high-intensity radiation at longer wavelengths.

An earlier theoretical study [2] of commercial spectroradiometers demonstrated a four order of magnitude stray

light contribution from wavelengths above the UV range of interest (290 – 440 nm), which would interfere with an accurate UV spectral intensity measurement. The same study proposed that implementing a digital micromirror device (DMD) could significantly reduce the impact of stray light using two techniques. The first involves leveling the dynamic range of the incoming radiation by selective wavelength modulation [2,3] where the undesired wavelengths are modulated at high frequency, creating an effective repetition rate, reducing their intensity and stray light contribution. The second method is to select a precise range of wavelengths using the DMD as an effective bandpass filter, where the longer wavelength radiation is not incident on the detector at all [2].

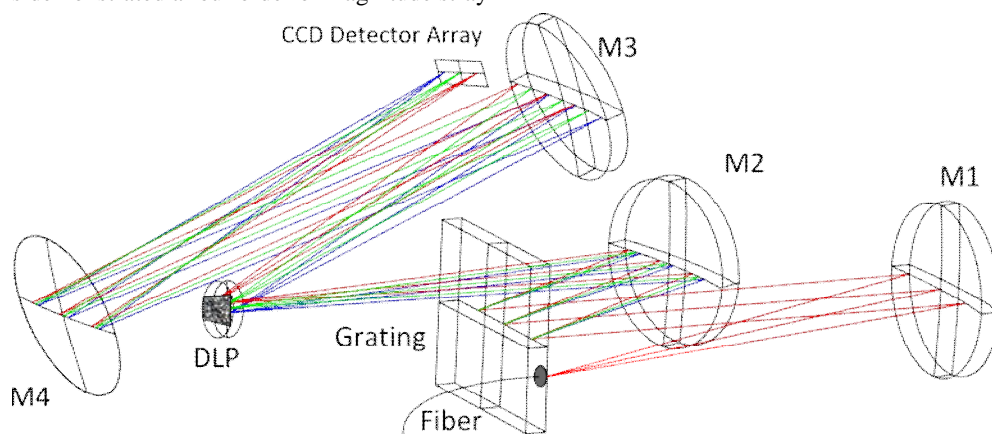


Figure 1. Optical design schematic of the μ -MUV prototype composed of 4 spherical mirrors (M1-M4), a 600 G/mm diffraction grating, DLP micromirror chip, and CCD detector array [4].

Based on a theoretical model constructed by optical modeling software [4], a physical prototype (μ -MUV Spectroradiometer) was assembled from off-the-shelf components. Optical layout of this prototype is presented in Figure 1. The prototype is composed of a fiber coupled light source, 4 spherical mirrors, a 600 G/mm diffraction grating, a 1024 x 720 pixel Extended Graphics Array (XGA) Digital Light Processor (DLP) micromirror chip [5], and a back-lit 2048 x 250 pixel Charge Coupled Device (CCD) detector array [6]. The use of off-axis spherics is exploited by creating a 1-dimensional spectral distribution on both the DLP chip and CCD array, where the detector array bins the vertical pixels. Each DLP pixel is controlled independently via an array of digital states of which there are three positions: the “float” position is not actively positioned and acts as a plane

mirror; the “on” position projects incident light vertically at an angle of 16.7° along the path of operation toward the CCD; the “off” position projects at an identical angle down and away from the optical path of the detection plane.

To compare the prototype to commercially available spectrometers, technical specifications such as spectral range, spectral resolution, and bandwidth were measured. The spectral range was tuned to the range 270 nm to 425 nm using the angular adjustment of the diffraction grating with a mercury pen lamp as a light source. The characteristic peaks of the pen lamp allowed for the definition of the wavelength scale and spectral distribution across the CCD array. Based on the number of illuminated CCD pixels and the defined spectral range, the resolution was determined to be 0.2 nm per

pixel. Lastly, the bandwidth of the spectrometer was determined to be 2.5 nm using the full width half maximum (FWHM) of an almost saturated peak of a 407 nm laser. More details of this prototype, operation, and characterization have been published in [7].

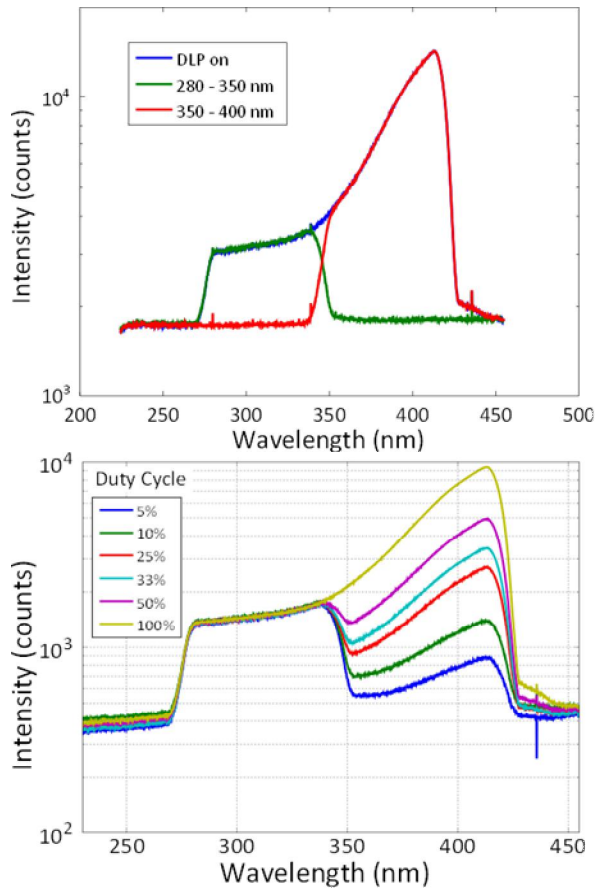


Figure 2. a) Spectral range selection demonstrated by choosing a range of DLP pixels in the “on” position. b) Longer wavelength light modulated via DLP “on”/“off” duty cycles to demonstrate dynamic range leveling and stray light reduction [7].

As a first effort in validating the stray-light reduction techniques proposed by Egli *et al*, a tungsten-halogen white light source was input and a range of the spectrum from 280 nm to 350 nm was selected by turning “on” corresponding pixels and can be seen in Fig. 2 a). Similarly, the range between 350 nm and 425 nm was separately selected. The data noted as “DLP on” represents the entire DLP chip in the “on” position and it is evident that the individually selected ranges are a good representation of the white light spectrum. The modeling, however, noted that removing longer wavelength radiation should result in reduced stray light contribution below 300 nm. Basic light-modulation techniques were implemented where half of the DLP was modulated at various duty cycles. The portion with longer wavelengths was chosen to flatten the dynamic range and reduce stray light in the shorter wavelength region. Duty cycles ranging from 5 % to 100 % are shown in Fig. 2 b), and as expected the intensity of the modulated region decreases proportionally with the duty cycle. As the duty cycle decreases however, the range in

the “on” portion from 290 – 350 nm subsequently decreases by a fraction of a percent. It is interesting to note that while the contribution in this range does demonstrate some stray light reduction, the reduction in amplitude of the background signal (430 – 450 nm) is more pronounced. While there was no orders of magnitude reduction in the stray-light intensity in the 270 nm to 320 nm region of interest during this first attempt, the basic principles of the spectral range selection and modulation to reduce the intensity are valid.

Despite the validity of the stray-light reduction techniques, the system itself has fundamental limits of operation due to the non-optimized nature of the prototype that may be limiting the detection capabilities. Perhaps the biggest limitation is the window on the DLP chip which only transmits 10 % of the UV radiation. Removal of this window is a delicate operation that requires special facilities so that no dust is generated and introduced to the micromirror system during the removal. Any contamination could reduce the functionality of the individual mirrors and, even worse, generate more stray light due to scattering off of a malfunctioning mirror or dust particle. If this risky operation is successful, exposure to atmospheric conditions would further introduce contaminants, so a sealed ultraviolet window, possibly CaF₂ or fused silica should be installed. Another limitation of the prototype is the “float” position which acts as a plane mirror, where light is passed horizontally through the system and potentially collected by the last mirror. Initially baffling attempts were installed and a 30 % broadband improvement was measured based on intensity measurements. Further reduction of stray-light from the DLP can be achieved by placing the undesired portion of the spectrum into the “off” position instead of the “float” position, replacing the foam baffling material with optically damping material, and possibly moving the CCD detector to a separate, isolated chamber. A new light-tight enclosure has also been designed and delivered to further enhance the reduction of stray light from external sources. Lastly, an air-cooled CCD detector array was provided in place of the desired actively cooled CCD system. Active cooling would improve the low-intensity radiation detection capability by reducing the dark-current signal present in the device, lowering the background signal.

While all of the above methods address the physical improvement of the prototypes measurement capability, software programming could improve the stray-light reduction techniques. As is evident in Figure 2 a), the spectrum could be reconstructed in a piecewise fashion by scanning small portions of the DLP pixels. By scanning narrow spectral ranges, the stray-light contribution from longer wavelengths would be reduced or eliminated. While scanning can increase the full spectrum acquisition time, there are many variables that can be used to improve the resolution of the prototype such as the wavelength window, scan step size, CCD integration time, number of scans to average, etc.

Thematic Network for Ultraviolet Measurements

Furthermore, due to the fast response of the mirrors and varying acquisition time of the CCD detector, the total acquisition time is likely much less than a double scanning monochromator. Another potential software improvement would be to use the acquired spectrum as feedback control for per pixel dynamic modulation to level the dynamic range as presented in the modelling [2].

With regards to characterizing the stray light incident on the CCD array, initial efforts using Schott-glass type filters indicated that the majority of stray light present was due to radiation greater than 550 nm. However, new methods of characterizing and correcting for stray-light in array spectroradiometers has been developed which uses a pulsed laser to characterize the in-range and out-of-range stray light responsivity of the detector [8]. A wavelength dependent stray-light correction matrix is then derived and applied to the array spectroradiometer acquired spectrum to correctly account for the stray-light contribution. Furthermore, we can use the DLP itself to characterize the stray light present in the system by examining the intensity of the light when the entire DLP is in the "off" position. By directing light away from the optical path, only stray light should be incident on the detector. While this measurement will contain no inherent spectral information, the total integrated intensity would allow for the subtraction from the acquired spectrum.

The μ -MUV Spectroradiometer prototype was assembled based on an optical model from off-the-shelf components yet has inherent limitations in its detection capabilities. Stray-light reduction techniques of spectral range selection and mirror modulation to reduce the dynamic range were validated experimentally, yet little stray-light reduction was detected. There are, however, many improvements to be made to the prototype including removal of the DLP window, replacing the CCD detector with an actively cooled detector, and a light tight enclosure which will improve the detection capabilities. Software improvements can enhance the stray-light

reduction techniques by scanning and reconstructing the spectrum and dynamic pixel modulation based on the acquired spectrum. Lastly, characterization of the stray light component of the acquired spectrum allows for better understanding and a path for future improvements.

Acknowledgements Part of this work has been supported by the European Metrology Research Programme (EMRP) within the joint research project ENV03 Traceability for Terrestrial Solar UV Irradiance Measurement (SolarUV). The EMRP is jointly funded by the EMRP participating countries within EURAMET and the European Union. Contribution of an agency of the U.S. government; not subject to copyright.

References

- [1] G. Seckmeyer, A. Bais, G. Bernhard, M. Blumthaler, S. Drüke, P. Kiedron, K. Lantz, R. L. McKenzie, and S. Riechelmann, GAW Report No. 191, *Instruments to Measure Solar Ultraviolet Radiation*, Part 4: *Array Spectroradiometers*, 41 (2010).
- [2] L. Egli, J. Grobner, M. Smid, G. Porrovecchio, T. Burnitt, K. M. Nield, S. Gibson, J. Dubard, S. Nevas, and M. Tormen, "New technologies to reduce stray light for measuring solar UV with array spectroradiometers," *AIP Conf. Proc.* **1531**, 825–828 (2013).
- [3] J. Rice, J. Neira, M. Kehoe, and R. Swanson, "DMD diffraction measurements to support design of projectors for test and evaluation of multispectral and hyperspectral imaging sensors," *Proc. SPIE* **7210**, 72100D-1–9 (2009).
- [4] T. Burnitt, "Optical Layout for Prototype DLP Spectrometer," (2012).
- [5] Texas Instruments Inc, *DLP 0.7 XGA 2xLVDS Type A DMD Technical Data Sheet* (2013).
- [6] Hamamatsu Inc, *CCD area image sensor Technical Data Sheet* (Hamamatsu City, Japan, 2012).
- [7] A. Feldman, T. Burnitt, G. Porrovecchio, M. Smid, L. Egli, J. Gröbner, and K. M. Nield, "Diode Array UV Solar Spectroradiometer Implementing a Digital Micromirror Device," *Metrologia* (in press).
- [8] S. Nevas, J. Gröbner, L. Egli, and M. Blumthaler, "Stray light correction of array spectroradiometers for solar UV measurements," *Appl. Opt.* **53**, 4313 (2014).

Characterisation of nonlinearities of array spectroradiometers in use for measurements of the terrestrial solar UV irradiance

Saulius Nevas¹, Peter Blattner², Omar El Gawhary³, Tomi Pulli⁴, Petri Kärhä^{4,5}, Luca Egli⁶, and Julian Gröbner⁶

1. Physikalisch-Technische Bundesanstalt, Braunschweig and Berlin, Germany
2. Federal Institute of Metrology, Bern-Wabern, Switzerland
3. VSL Dutch Metrology Institute, Delft, The Netherlands
4. Aalto University, Espoo, Finland
5. Centre for Metrology and Accreditation MIKES, Espoo, Finland
6. Physikalisch-Meteorologisches Observatorium Davos, World Radiation Center, Davos, Switzerland

Abstract

Terrestrial solar UV irradiance varies over 5 to 6 orders of magnitude. A respective linearity characterization of array spectroradiometers is required by the measurement application and was one of the tasks within the EMRP “SolarUV” project. Within this framework, different setups at Aalto, METAS, PTB and VSL have been applied. We present technical realizations of the setups and results of comparison measurements that were carried out for validation of the methods.

Introduction

Terrestrial solar UV irradiance varies within the relatively narrow spectral range, 280 – 400 nm, over a large dynamic range, 5 to 6 orders of magnitude. Hence, a linear dependence between the measured solar UV irradiance values over the whole dynamic range and the respective signals of a spectroradiometer that is used for the measurements is required, i.e., the linearity of the instrument must be known. Residual deviations from the linear regime will yield errors both in absolute values as well as in relative spectral distributions of the measured solar UV irradiance.

In the case of compact array spectroradiometers, the linearity of the CCD instrument is typically characterised by exposing the instrument to the radiation of a stable source and varying the integration time of the detector.

This is a simple but by far not complete characterization method. In fact, it accounts for the linearity of the signal processing electronics only. In principle, the linearity of such devices should be tested by varying the spectral irradiance level over the whole dynamic range. For the radiometric characterisation of the linearity of the spectroradiometers, the technical challenge consists in providing a radiation source, the spectral irradiance of which can be dynamically tuned over 5 to 6 orders of magnitude. In the case of, e.g. halogen lamps, used for the calibration of the instruments, this is difficult.

Within the framework of an EMRP ENV03 project “Traceability for surface spectral solar ultraviolet radiation”, an approach to the linearity characterisation of array spectroradiometers used for the solar UV radiation measurements has been chosen based on monochromatic sources with different setups at Aalto, METAS, PTB and VSL. This paper presents technical realisations of the setups. A comparison of the linearity measurements using the setups of the NMIs was carried out in early spring 2014. These results are presented. As an outcome of these activities, a mobile and validated device was available for the linearity characterisation of array spectroradiometers of participants taking part in the UV intercomparison at PMOD/WRC, Davos, Switzerland in July 2014.

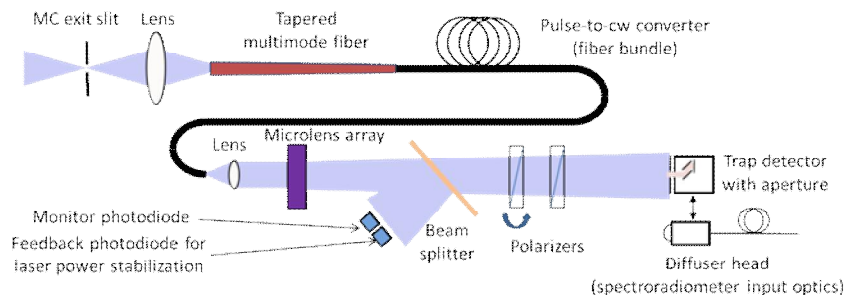


Figure 1. Beam conditioning in the TULIP setup at PTB for linearity characterization.

Measurement setups

At PTB, a wavelength tuneable laser facility (TULIP) was used for the purpose of the linearity characterisations of array spectroradiometers. The TULIP facility was extended into the solar UV spectral range by frequency doubling and tripling of a mode-locked Ti:Sa fs-laser [1]. A beam conditioning unit was developed providing a stable, depolarised, spectrally narrow and spatially

uniform irradiance field. Schematics of this beam preparation unit are shown in Fig. 1. A specially designed fibre bundle used within the beam conditioning unit acts as a pulse-to-cw converter. A continuous wave (cw) nature of the radiation is important for the linearity characterisation of the instruments. Spectral irradiance levels up to $1 \text{ W m}^{-2} \text{ nm}^{-1}$ can be set and attenuated by a variable filter. The measurements were accomplished relative to a trap detector made of S1227 photodiodes.

Thematic Network for Ultraviolet Measurements

A quasi-cw laser similar to that used at PTB was also used at METAS. The beam is directly applied to the entrance optics of spectroradiometers. The power level is changed by adjusting the working point of a liquid crystal modulator and adding attenuation filters.

Aalto built a setup based on a single monochromator with two light sources. A 500-W Xe-lamp provides a smooth spectrum to carry out measurements over the UV region. A 1-kW Hg-lamp is used to provide higher intensities. The light exiting the monochromator is collimated and attenuated with interchangeable neutral-density filters in two consequent filter wheels (see Fig. 2). The light beam then continues to the device to be characterized through a beam splitter taking a fraction of the beam to a photodiode serving as the linearity reference. Intensity levels have been set so that the photocurrent of the S1337 photodiode keeps in its linear region [2].

VSL developed a portable system for in-situ characterisation of spectroradiometers (see Fig. 3). The device consists of two linear polarizers, whose reciprocal transmission axes can be set to any angle by a rotation mount, a 2-inch averaging sphere and a reference Si

detector (S1226-44BQ) positioned at one of the output ports of the sphere, acting as the linearity reference. The system is currently powered by a UV laser at 372.7 nm, but in principle other sources can also be used.

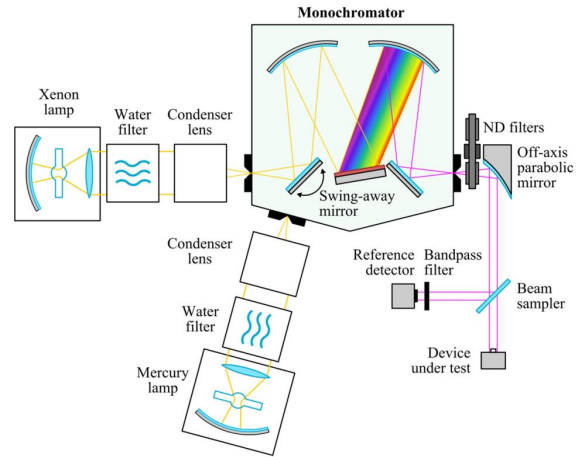


Figure 2. Setup for linearity measurements at Aalto University.

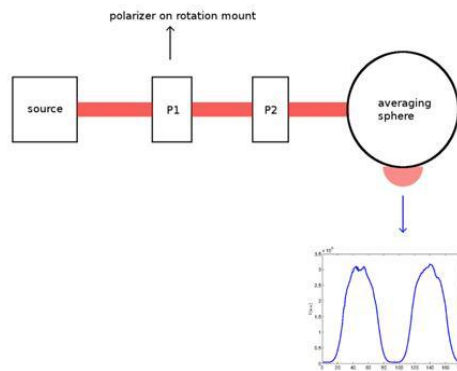


Figure 3. Picture and schematic diagram of the setup for linearity measurements built at VSL.

Results

A number of spectroradiometers were characterized within the “SolarUV” project. Here we present results for two instrument used to compare the performance of the different setups.

AvaSpec-ULS2048LTEC-USB2

The AvaSpec consists of a cooled CCD with 2048 pixels, and has 16 bit resolution. It operates over the wavelength range of 200 nm – 1100 nm, has 2.4 nm bandpass, and the dispersion is 0.6 nm/pix. The entrance optics consist of a 200 μm multimode fiber with a diffuser head.

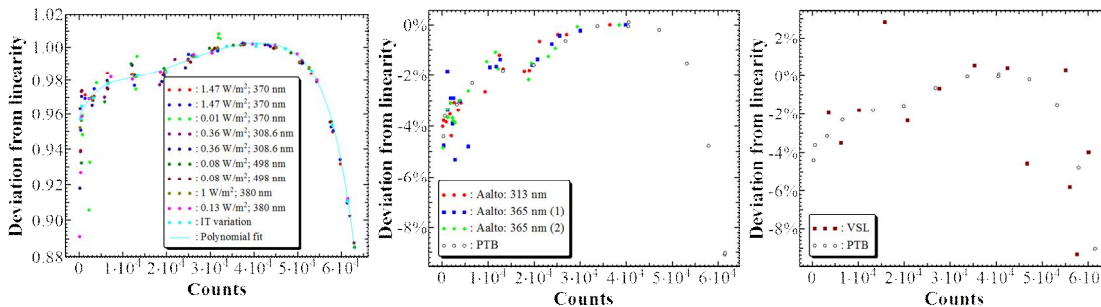


Figure 4. Nonlinearities measured for the AvaSpec spectroradiometer at a) PTB, b) Aalto and c) VSL. Corresponding values of PTB have been included to Figs. b) and c) to demonstrate the agreement.

The nonlinearities calculated from raw signals measured at various institutes are presented in Figs. 4 a) – c).

Results of the linearity measurements are in a good agreement. The wavelength dependence appears

negligible. PTBs results were measured with two different methods. 1. Keeping the signal level fixed and varying the integration time, and 2. varying the irradiance level. Both methods gave similar results.

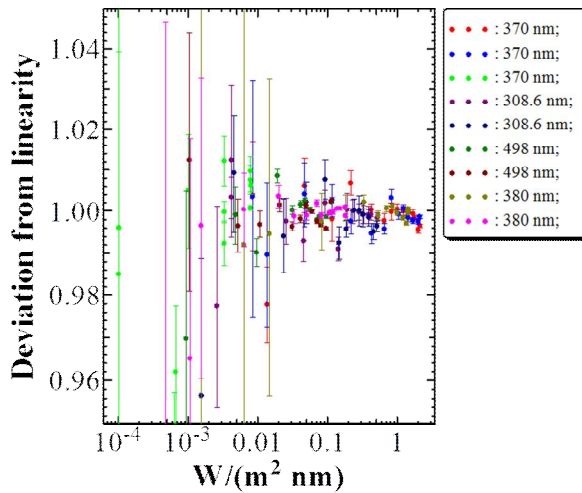


Figure 5. Results of PTB after applying a polynomial correction to the measured non-linearity as a function of ADC counts.

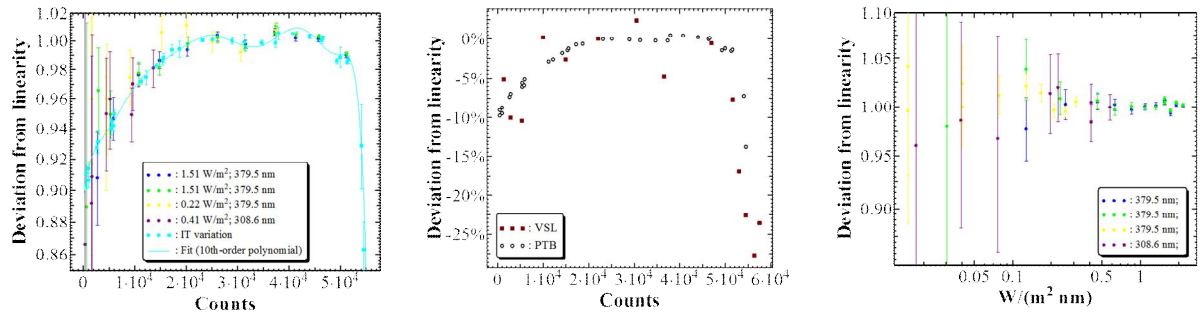


Figure 6. Nonlinearity of the Stellarnet spectroradiometer as measured by a) PTB and b) VSL. c) Results of PTB after polynomial correction for the measured non-linearity.

Conclusions

Two different array spectroradiometers were characterized to compare setups for the linearity characterizations at Aalto, PTB and VSL. The measurements in irradiance-variation mode could be carried out within a dynamic range from $1 \cdot 10^{-4} \text{ W m}^{-2} \text{ nm}^{-1}$ to $2 \text{ W m}^{-2} \text{ nm}^{-1}$ and from $0.01 \text{ W m}^{-2} \text{ nm}^{-1}$ to $2 \text{ W m}^{-2} \text{ nm}^{-1}$ with the AvaSpec-ULS2048LTEC and the Stellarnet spectroradiometers, respectively. The lowest measurable irradiance was limited by the responsivity of the instruments.

Results of the linearity measurements were in a good agreement. Also results obtained by irradiance variation were consistent with those collected by varying the integration time of the instruments.

Both instruments showed noticeable nonlinearities that seemed to be caused by signal processing electronics (ADC) and could be corrected as a function of ADC

The instrument shows noticeable nonlinearities that seem to be caused by signal processing electronics (ADC) and could be corrected as a function of ADC counts. Figure 5 shows the results of PTB after applying a correction for the measured non-linearity. Having this correction applied, no additional nonlinearity for irradiances of up to $2 \text{ W m}^{-2} \text{ nm}^{-1}$ could be detected.

Stellarnet Blue-Wave spectrometer

The Stellarnet spectroradiometer utilized an uncooled CCD, with 2048 pixels, and 16 bit resolution. The wavelength range is 280 – 410 nm, and the dispersion is 0.06 nm/pix. A 600 μm multimode fiber with a diffuser head was attached during the characterizations at Aalto and PTB. At VSL, the device mounts directly to a port in the sphere.

The results of PTB and VSL are presented in Figs. 6 a) – c). They are very similar to the results obtained for the AvaSpec spectroradiometer.

counts. Having this correction applied, no additional nonlinearity for irradiances of up to $2 \text{ W m}^{-2} \text{ nm}^{-1}$ could be detected.

Acknowledgement Part of this work has been supported by the European Metrology Research Programme (EMRP) within the joint research project ENV03 “Traceability for surface spectral solar ultraviolet radiation” (SolarUV). The EMRP is jointly funded by the EMRP participating countries within EURAMET and the European Union.

References

[1] S. Nevas, J. Gröbner, M. Schuster, P. Sperfeld, L. Egli, G. Hülsen, A. Sperling, P. Meindl, S. Pendsa, and S. Pape, “Calibration of the reference spectroradiometer for the quality assurance of the terrestrial solar spectral ultraviolet radiation measurements in Europe,” *Proceedings of the Newrad 2014*, pp. 9–10 (2014).
 [2] T. Kübarsepp, A. Haapalinna, P. Kärhä, and E. Ikonen, “Nonlinearity measurements of silicon photodiodes,” *Appl. Opt.* **13**, 2716–2722 (1998).

Application of a dual-channel solid state spectrometer to measure spectral radiation and atmospheric constituents

Andrew R.D. Smedley, Richard C. Kift, and Ann R. Webb

University of Manchester, School of Earth, Atmospheric and Environmental Sciences, United Kingdom

Introduction

The state of the art instrument for measuring solar radiation at the earth's surface is the traditional scanning spectroradiometer, and its derivatives such as Brewer spectrophotometers. However such instruments suffer some disadvantages: high cost (~€100k), susceptibility to movement, and speed of operation.

Solid state (CCD and photodiode) instruments however are relatively inexpensive, stable and acquire data over a wide wavelength range simultaneously. The disadvantages of these newer instruments include their reduced response at the shortest wavelengths, smaller dynamic range and, due to the intrinsic single-monochromator design, susceptibility to stray light.

As part of the European Metrology Research Programme (EMRP) Project ENV03 "Traceability for surface spectral solar ultraviolet radiation," researchers at the University of Manchester are investigating the performance of a dual channel spectrometer system in conjunction with a stand-alone solar tracker in an atmospheric monitoring setting. The deployed system is monitoring simultaneous measurements of direct and global spectral irradiance over a period of several months. By measuring both quantities simultaneously the instrument can provide wavelength-integrated radiometric quantities such as erythemally-weighted UV, PAR, etc., separated into direct, global and diffuse components and additionally these can be processed to derive a continuous data series of ozone, AOD and potentially other absorbing species – with minimal data loss due to scanning and sampling issues.

Instrument description

The METCON spectrometer system used in this study is mounted in a city centre location, on the roof of a 35 m high building (Fig. 1), giving it a relatively unobstructed view of the horizon. The core instrument consists of a pair of nominally identical 15-bit spectrometers. These are mounted alongside each other together with common data acquisition electronics within a temperature stabilised container. Each spectrometer channel is connected to its respective entrance optics via a separate 5 m long 600 μm diameter optical fibre. The individual monochromators use a 512 pixel diode array detector covering the UV-A, UV-B and visible spectral range (280 – 700 nm) with a spectral resolution of 2.2 nm.

One spectrometer channel receives its input from a global irradiance (cosine response) entrance optics, mounted horizontally at a height of approximately 1.3 m. The second channel receives its input from a direct sun optic mounted upon a sun-tracker. The direct sun optic is formed from a baffled tube, the front entrance of which is

protected by a fused quartz window and angled cover to prevent water ingress. At the rear of the tube, to reduce the incoming signal, a ground quartz disc is mounted behind the final baffle and in front of the entrance to the optical fibre. The two baffles at either end of the direct sun optics define the field of view (FOV) of the entrance optic. The suntracker upon which the direct sun optic is mounted has a pointing accuracy of $<0.01^\circ$, and additionally makes use of a four quadrant photodiode detector to ensure the sun remains in the FOV of the detection optics without the requirement of any additional computer control.

The core instrument is housed within a weatherproof aluminium container, lined internally with polyethylene insulation (thermal conductivity, $k = 0.044 \text{ W/m}\cdot\text{K}$). The temperature of the system is maintained by way of an air-to-air active thermo-electric cooling system under proportional-integral-derivative controller (PID) control. The PID parameters were determined using the method proposed by Ziegler and Nichols [1]. Using PID parameters chosen in this way laboratory tests for ambient temperatures in the range of -20°C to $+34^\circ\text{C}$ confirmed that the instrument set-point can be maintained to within $\pm 0.01^\circ\text{C}$ during stable conditions and within $<0.05^\circ\text{C}$ for rapid changes in ambient temperature ($\sim 1^\circ\text{C}/\text{min}$).



Figure 1. METCON dual channel spectrometer system deployed at Manchester Surface Radiation Monitoring Site.

One disadvantage of array spectrometers is their limited dynamic range in comparison to PMT based scanning systems. A method to overcome this is to select an integration time where the array is not quite saturated. Usually there is no prior knowledge of the signal to be measured so that a two stage methodology is required. First a measurement at a short integration time is taken; this is then used to make an estimate of the ideal integration time in the second measurement [2]. For a dual channel instrument as in this study where a single

data acquisition command results in spectra being recorded on both arrays, the situation is more complicated as the integration time must be chosen so that neither channel is saturated. Rather than continually adjust the integration time for changing atmospheric signal, here a short fixed integration time of 25 ms is used for field measurements. This has the advantages that many repeated unsaturated spectra can be averaged to increase the signal to noise ratio, requires no settling time and is operationally simple. For the METCON spectrometer system the signal averaging is split between onboard averaging carried out by the data acquisition electronics and software averaging. This methodology permits us to average approximately 400 individual spectra over a period of 55 s and save a single averaged spectrum for each channel every 1 min.

Instrument characterization and calibration

For a typical scanning instrument initial wavelength calibration is usually carried out via a high frequency scan of known lamp emission lines to determine their peak. However by their design this is not possible for array instruments with only a small number of pixels defining the measured line shape, depending on oversampling. Care must be taken then in order to choose the best method to determine the sub-pixel location of the measured emission peak. Here we use the centroid method after Shortis, Clarke and Short [3] and once the sub-pixel peak locations had been determined, a third order polynomial fit was applied using the least-squares method.

The emission spectra used were from a simultaneous measurement of a Hg(Ar) and Ne gas discharge pencil lamps. This combination of lamps provided 5 single lines across the instrument's wavelength range, and a further 3 multiple lines were included by weighting individual line intensities. All emission line wavelengths taken from the NIST Atomic Spectra Database (<http://www.nist.gov/pml/data/asd.cfm>, 2012). Both direct and global irradiance channels showed no pattern in the residuals and the r.m.s. difference was at the level of 0.05 nm. Further refinement to the wavelength calibration is carried out by reference to Fraunhofer line structures observable in solar spectra measured in the field.

One of the principle limitations of array instruments is that being based upon single monochromators, stray light remains an issue, particularly for the solar UV spectral region. To address this problem we follow Kreuter and Blumthaler [4] who demonstrated the validity of Zong et al's [5] approach in this application using a simplified experimental setup requiring only a single laser at 405 nm. In brief the concept is as follows. The measured spectrum, \mathbf{Y}_{meas} , can be considered the sum of the instrument's in-band response, \mathbf{Y}_{IB} (within the spectral line spread function) and the stray light contribution, \mathbf{Y}_{SL} . The stray light contribution can be calculated from matrix multiplication of the stray light distribution function, \mathbf{D} , with the in-band response, so that

$$\mathbf{Y}_{\text{meas}} = \mathbf{Y}_{\text{IB}} + \mathbf{Y}_{\text{SL}} = [\mathbf{I} + \mathbf{D}] \cdot \mathbf{Y}_{\text{IB}} \quad (1)$$

and, solving for the in-band response

$$\mathbf{Y}_{\text{IB}} = [\mathbf{I} + \mathbf{D}]^{-1} \cdot \mathbf{Y}_{\text{meas}} = \mathbf{C} \cdot \mathbf{Y}_{\text{meas}} \quad (2)$$

where \mathbf{I} is the identity matrix and \mathbf{C} is the stray light correction matrix. Additionally there is a stray light contribution from wavelengths outside of the instrument's detectable range which is accounted for by adding a constant term, determined separately for solar and quartz halogen sources.

To apply the stray light correction practically three options were considered for the stray light distribution matrix. First using the normalised, dark-subtracted counts as measured for wavelengths outside the in-band region. Second an analytic power function

$$\text{SDF}(\lambda, \lambda_0) = c + b \cdot |\lambda - \lambda_0|^{-a} \quad (3)$$

and finally a model-based parameterisation based on the theoretical line spread function for a diffraction grating monochromator given by Sharpe and Irish [6]. Comparing the goodness of fit of the analytic power function and the model-based parameterisation we find that the model-based parameterisation performs much better with r.m.s. differences of 5.86×10^{-6} versus 1.10×10^{-4} for the analytical power function (Fig. 2). Testing all three options for the SDF using measurements of quartz halogen lamp with a WG320 cut-off filter placed between lamp and detector showed that the analytic power fit performed best, reducing counts in for $\lambda < 320$ nm to almost zero. The discrepancy for the raw counts-based SDF and model-based parameterisation is attributed predominantly to the differences in the three SDF functions at wavelengths > 100 nm from the laser line.

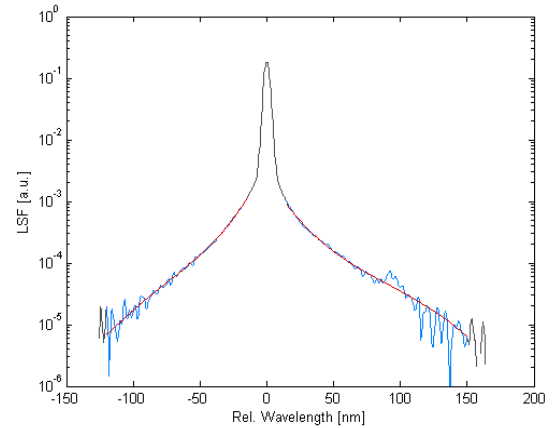


Figure 2. LSF plot showing model-based parameterisation fit (red line) for channel B. Blue line shows measured LSF.

A further useful characteristic of the ability of array spectrometers is the noise equivalent irradiance (NEI), defined as the standard deviation of the dark spectra divided by the instrument's responsivity). For the direct sun channel, operating with repeated measurements at an integration time of 25 ms, this is found to be $< 0.1 \text{ mWm}^{-2}\text{nm}^{-1}$ for wavelengths above 300 nm and $< 0.04 \text{ mWm}^{-2}\text{nm}^{-1}$ for wavelengths above 315 nm. (Fig. 3). For

Thematic Network for Ultraviolet Measurements

the global irradiance channel the values are approximately an order of magnitude greater due to the reduced throughput. Applying the stray light correction as described to sample atmospheric spectra we find also that stray light is removed as expected at wavelengths <290 nm, leaving only noise at the level of the *NEI*.

Turning to the absolute calibration for both channels, this was carried out with respect to a current-controlled NIST-traceable 1 kW quartz halogen lamp. Before the instrument was transferred to the monitoring site a reference measurement was performed for each channel with a 200 W transfer standard lamp housed within a field transportable calibration unit. During the monitoring period both channels responsivity was checked by repeating measurements of the 200 W transfer standard at intervals of 2 to 5 weeks.

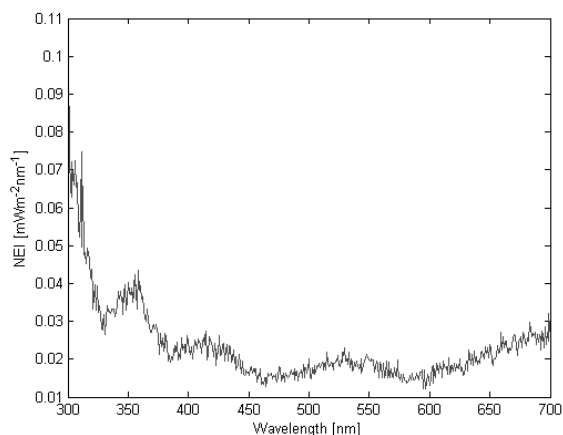


Figure 3. Noise Equivalent Irradiance for channel B (direct sun).

Although the instrument housing is temperature stabilised to ± 0.01 °C under normal operating conditions, the effect of temperature on the instrument characteristics was also investigated. In turn the temperature was set at intervals of 1 °C over a range of $\pm 2^\circ$ around its operating set-point and after a period of stabilisation, the following spectra were recorded: dark counts, measurements of Hg(Ar) and Ne emission lamps, and of a quartz halogen lamp. From these spectra the mean thermal wavelength shift was found to 0.002 nm/°C and over most of the spectral range the relative change in responsivity is <0.1 %/°C, although this increases to 3 %/°C at 290 nm. The dark counts increase by 15 counts/s per degree of temperature rise, equivalent to 1.5 mWm⁻²nm⁻¹ at 290 nm and 0.2 mWm⁻²nm⁻¹ at visible wavelengths. In practice these thermal effects should be approximately 2 orders of magnitude smaller and therefore not unduly affect the data produced.

The raw data produced by the instrument is denoted level 0 data and has had no processing applied, except for averaging. To produce calibrated spectra for both channels a number of steps are necessary. The first of these is to subtract dark counts. As the instrument has no internal shutters, datum dark count spectra are recorded as part of the calibration process.

After dark subtraction, solar spectra from both channels are scaled to units of counts/s before correcting them for stray light using a stray light distribution matrix based on an analytic power function as discussed above.

The dark and stray light corrected spectra are then converted to level 1 calibrated spectra by applying the responsivity (calculated from measurements of the quartz halogen lamps, and also corrected for dark and stray light effects). Throughout the wavelength grid used is that defined by the pixel locations.

Finally level 1 spectra for both direct and global irradiance channels are passed through a wavelength, bandwidth and wavelength resolution homogenisation function using the solar Fraunhofer structure to produce level 2 data.

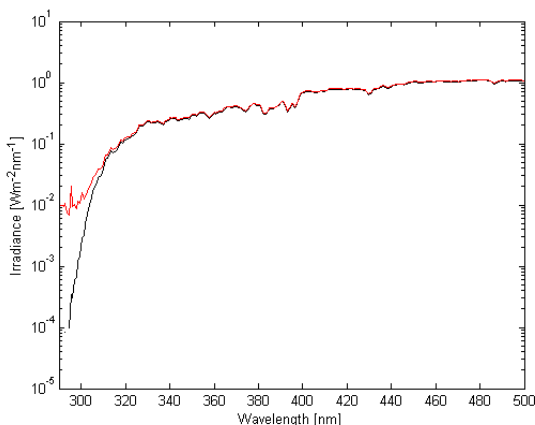


Figure 4. Example plot of stray light correction for direct sun spectrum. Red line shows calibrated and dark corrected spectrum; black line shows the same spectrum with additional stray light correction.

Results

Figure 4 shows an example direct midday spectrum, with and without stray light correction applied. It can be seen that the specified correction procedure removes stray light contamination at the shortest wavelengths, with residual noise of 0.1 mWm⁻²nm⁻¹ in line with that expected from the measured noise-equivalent irradiance.

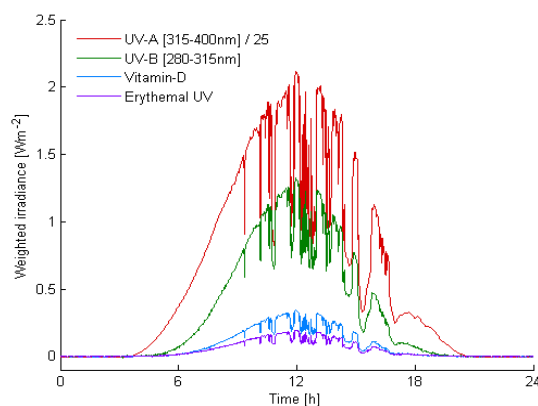


Figure 5. Example weighted quantities during day 154 of 2013, in Manchester, UK.

Accurate measurement of the irradiance at the shortest wavelengths is critical in solar UV measurements, particularly if it is planned to integrate over biological active weighting functions, such as for erythema or for Vitamin D production. Once stray light has been removed and the raw spectrum calibrated for both wavelength and in an absolute sense, the irradiance can be integrated over multiple wavebands (Fig. 5). One of the strengths of this instrument can be seen here: provided the calibrated spectra are available, many different types of weighting can be calculated for simultaneous time periods with no limitation due to number of detectors (such as in a multi-filter instrument). Further, should new action spectra prove useful in the future there is also the capability to process historic data. However it should be noted that a detectability limit of $0.4 \text{ mWm}^{-2}\text{nm}^{-1}$ limits the accuracy of short wavelength biased weighted quantities at larger solar zenith angles.

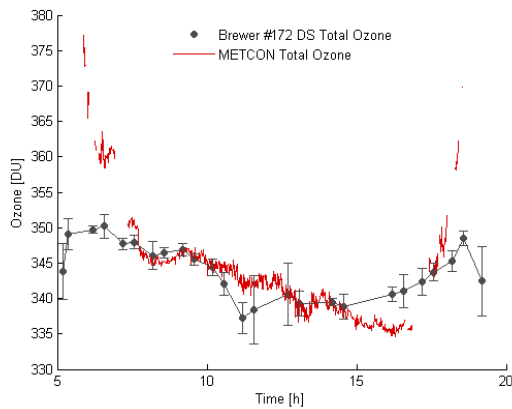


Figure 6. Selected clear day total ozone column retrieval during June 2013 (red line) vs Brewer 172 (black markers).

The advantage of the direct sun channel lies not only in being able to split ground-level radiation into direct, diffuse and global components, but also to retrieve column integrated amounts of trace atmospheric absorbers. Typically retrieval of such atmospheric constituents is done using differential optical absorption spectroscopy, by application of the Lambert-Beer Law

$$I(\lambda) = I_0(\lambda) \cdot \exp(-\alpha(\lambda)Xm_u - \beta(\lambda)\frac{P_s}{p_0}m_R - \delta(\lambda)m_a) \quad (4)$$

where the three terms relate to absorption by ozone, Rayleigh scattering, and extinction by aerosols, respectively. The relatively wide slit function (FWHM = 2.2 nm) of this instrument however masks much of the small scale structure evident in the ozone absorption cross-section spectrum. The first step is to calculate the total optical depth of the atmosphere by reference to an extra-terrestrial spectrum, and then remove the effect of Rayleigh scattering and aerosols by fitting a fourth order polynomial over the wavelength range of 340 to 700 nm. The remaining extinction is predominantly due to ozone, although there is a small contribution from SO₂ and other trace gases. To minimise the effects of these other absorbers on the total ozone column (TOC) retrieval a

robust regression is applied using data between 314 nm and 327 nm. Data are filtered according to maximum direct irradiance and for retrieved TOC that exhibit a standard deviation < 2.5 DU over 3 minute intervals. This second criterion is chosen to match that typically used by Brewer spectrophotometers in identifying values affected by clouds. Figure 6 shows an example day of TOC retrieved from the direct sun channel of the METCON instrument against direct sun measurements from a co-located Brewer (#172). During the central period of the day the r.m.s difference between the values obtained with the METCON compared to Brewer #172 is < 0.8 %, whilst including all valid data for the day raises this to approximately 1.3 %. There is some evidence of airmass dependence; also evident is the increased temporal resolution from the array spectrometer system.

Once the TOC for an individual spectrum has been calculated, this can be reinserted into the Lambert-Beer Eq. (4) along with estimates for Rayleigh scattering, to determine values for aerosol optical depth at all wavelengths. Additionally the second stage of the DOAS algorithm includes cross-sections for SO₂, NO₂, BrO, CH₂O, but the retrieval of these is at present limited by some residual structure likely due to instrument bandwidth issues.

Summary

A dual channel array-based spectrometer offers a novel alternative for measuring simultaneous direct sun and global irradiance. The instrument temperature can be controlled at the level $\pm 0.01 \text{ }^\circ\text{C}$ and laboratory characterisation of the wavelength calibration can reach accuracy of 0.05 nm (equivalent to 0.06 pixels). Averaging at a short integration time, suitable for an instrument in a monitoring scenario, results in an NEI of $0.04 \text{ mWm}^{-2}\text{nm}^{-1}$ for wavelengths > 315 nm on the direct solar channel, and $0.4 \text{ mWm}^{-2}\text{nm}^{-1}$ for global irradiance spectra. The stray light correction methodology based upon an analytic power function successfully removes stray light, leaving only noise at the level of the NEI. We also note that using both the measured stray light distribution and a model-based parameterisation for the stray light function do not remove the stray light as efficiently.

Calibrated global irradiance spectra corrected for stray light enable high frequency time series of many different weighted quantities to be calculated with reasonable accuracy in addition to the spectra themselves. The addition of a second channel has the advantage of permitting calculation of direct and diffuse quantities and retrieval of total ozone column and aerosol optical depth. Although example clear days indicate agreement between the METCON instrument and ozone retrieved from a Brewer spectrophotometer at the level of 1 %, improved retrievals of other trace gases are limited by residual structure related to the instrument bandwidth. However incorporating more advanced array spectrometers with improved detection at UV wavelengths and narrower bandwidths into a similar set-up promises to overcome these issues.

Acknowledgement This work has been supported by the European Metrology Research Programme (EMRP) within the joint research project ENV03 “Traceability for surface spectral solar ultraviolet radiation” (SolarUV). The EMRP is jointly funded by the EMRP participating countries within EURAMET and the European Union.

References

- [1] J.G. Ziegler and N.B. Nichols, “Optimum settings for automatic controllers,” *Trans. ASME*. **64**, 759–768 (1942).
- [2] M. Blumthaler, J. Gröbner, L. Egli, and S. Nevas, “A Guide to Measuring Solar UV Spectra using Array Spectroradiometers,” *AIP Conf. Proc.* **1531**, 805–808 (2013).
- [3] M.R. Shortis, T.A. Clarke, and T. Short, “Comparison of some techniques for the subpixel location of discrete target images,” *Proc. SPIE*. **2350**, 239–250 (1994).
- [4] A. Kreuter and M. Blumthaler, “Stray light correction for solar measurements using array spectrometers,” *Rev. Sci. Instrum.* **80**, 096108 (2009).
- [5] Y. Zong, S.W. Brown, B.C. Johnson, K.R. Lykke, and Y. Ohno, “Simple spectral stray light correction method for array spectroradiometers,” *Appl. Opt.* **45**, 1111–1119 (2006).
- [6] M.R. Sharpe and D. Irish, “Stray Light in Diffraction Grating Monochromators,” *Opt. Acta*. **25**, 861–893 (1978).

Multi-spectral UV sky camera: MUSKY

V. Caricato¹, A. Egidi¹, M. Pisani^{1,*}, M. Zucco¹, and M. Blumthaler²

1. Istituto Nazionale di Ricerca Metrologica, Torino, Italy, * m.pisani@inrim.it
 2. Innsbruck Medical University, Biomedical Physics, Innsbruck, Austria

We present an instrument to measure spectral irradiance of sky based on a multispectral camera and a fisheye catadioptric imaging system. The purpose of the prototype is to improve the traceability of UV radiometers to SI units. The design, the realization, and the calibration of the device are presented.

Introduction

Commercial UV radiometers observe the 2π emissivity of sky in the UV region through integrating entrance optics and measure the total irradiance. This parameter is particularly important for monitoring skin cancer risk (UV index). Traceability of such instruments to SI units is so far not guaranteed. Dependence of entrance optics with angle (cosine effect) and environmental variables, such as presence of clouds, seriously affect the accuracy of UV radiometers. In order to measure the corrections and implement a valid model of the emissivity of the sky measured by radiometers it is important to realize an instrument used as a reference which collects as much information as possible of spectral and spatial distribution of sky irradiance.

In the framework of the European Metrology Research Program (JRP ENV-03 SolarUV), we have realized a camera, based on a large convex spherical mirror coupled with quartz lens objective and a special CCD sensor, capable of observing the whole sky (up to 83° zenith angle). The spatial resolution is better than 1 square degree per pixel. A filter wheel made with 11 band pass filters allows generating the irradiance spectrum of the light coming from each direction. Compared to classical spectrogoniometers the instrument generates a complete spectral map of the sky in few seconds allowing dynamic sky monitoring and thanks to its compactness can be easily transported allowing in situ calibrations.

Realization

The Multi-spectral UV sky camera (MUSKY) is based on a UV sensitive CCD Camera equipped with a motorized filter wheel holding 11 filters having 10 nm nominal width and being uniformly distributed in the 300 – 400 nm range (see Fig. 1). The aluminum filter holder is designed to maximize compactness in order to reduce the impact of the reflected image of the camera in the sky image. The filter wheel is enclosed in a compact aluminum box (blackened inside and reflecting outside) and is moved by a step motor which in a fraction of a second positions precisely the filter in front of the objective.

The mirror was made from glass, and it is coated with aluminum protected with quartz. The diameter of the mirror is 300 mm and the curvature radius is 262 mm. The objective of the camera is made from quartz lenses. The base of the instrument is a honeycomb plate on

which the mirror is placed and a frame made from aluminum is fixed to hold the camera in the right position. The complete structure can be mounted on a tripod. A scheme of the instrument is shown in Fig. 2.

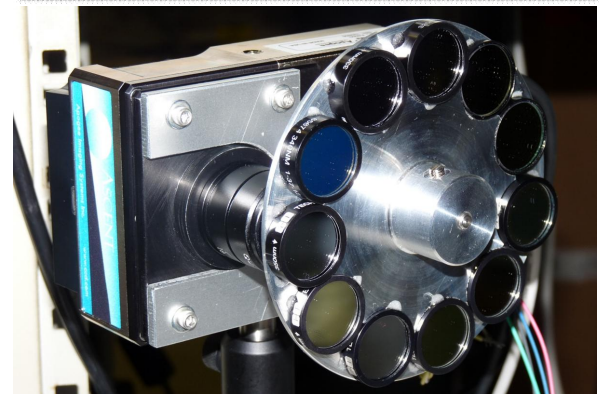
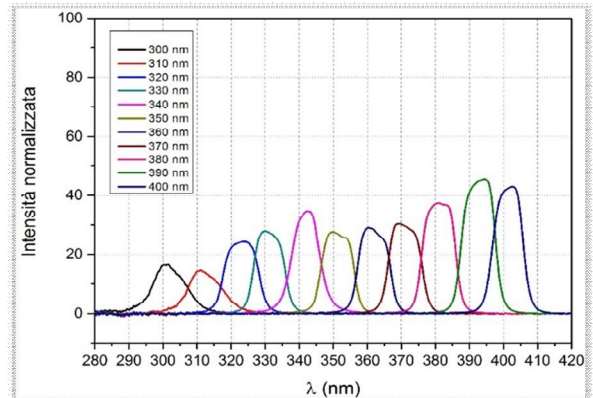


Figure 1. Transmittances of the band-pass filters (a) mounted on a motorized filter wheel (b) designed to minimize the shadow created by the camera itself.

Calibration

The instrument has been calibrated for its spectral response and for spatial response. The MUSKY has been compared with a reference spectrogoniometer installed on the roof of Innsbruck Medicine University. The MUSKY has acquired several series of multispectral pictures and at the same time the reference spectrometer acquired a multitude of spectra in different portions of the sky (Fig. 3). Later the results have been elaborated by comparing the portion of the multispectral images corresponding to the portion recorded by the reference instrument at about the same time. The reference spectra have been resampled and weighted in order to have the same measurement spectral interval as MUSKY and the two curves are compared. The ratio of the two curves gives the calibration factor for each wavelength and each zenith angle. The variability obtained with the process is of the order of 10 % and can be mostly due to the non-ideal temporal coincidence of the measurements.

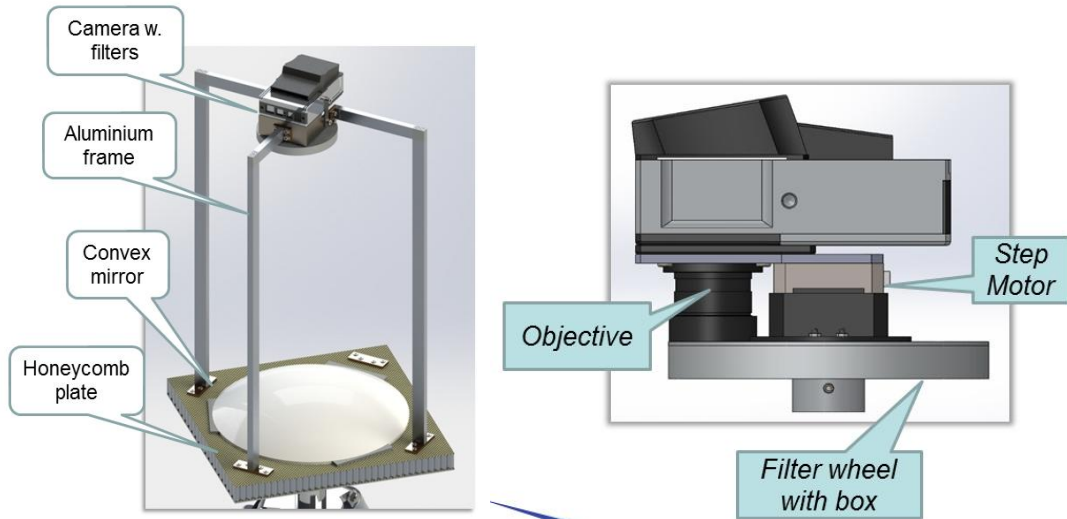


Figure 2. Structure of the assembled instrument (left) with a detail of the camera assembly (right).

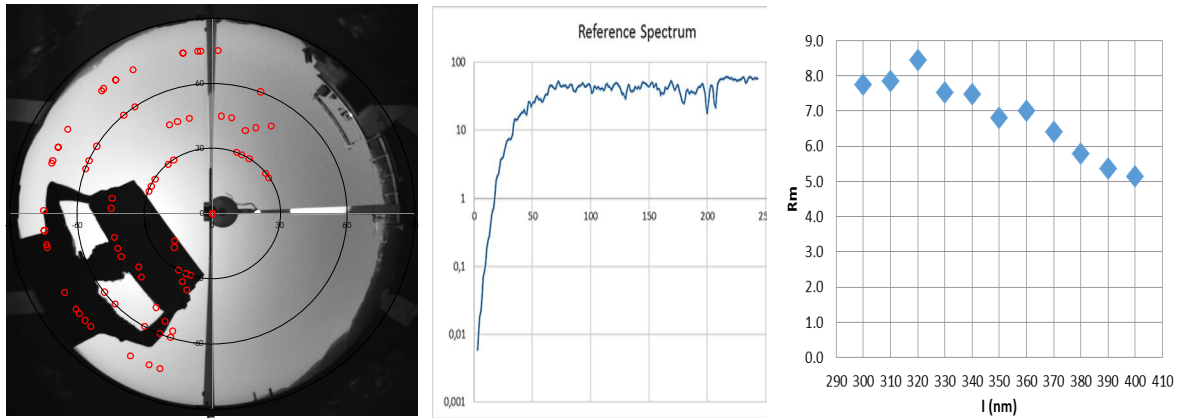


Figure 3. Left: one of the images taken with the Musky with the position acquired with the reference spectrometer (red dots). Center: one of the reference spectra. Right: the ratio of the measurements allows to generate the calibration function (right).

Further spectral calibration will be carried out in the laboratory with an LDLS source. Spatial response has been calibrated by geometrical considerations supported by experimental realizations. The angle to pixel conversion matrix has been built with an uncertainty less than 1° .

Dynamic range

The dynamic range is limited by the CCD and the camera (Ascent 4000 equipped with cooled Kodak KAI

4022 sensor). Because of the different responsivity versus wavelength and the variation in sky emissivity, the intensity of the image changes by a factor 100 or more. To compensate this while keeping good dynamic range for each image, acquisitions at different exposure times are recorded. In Fig. 4 a typical recording set is displayed. From this, the spectrum of each of the ~ 30 kpixel of the image is obtained by the combination of the three series normalized for the exposure time.

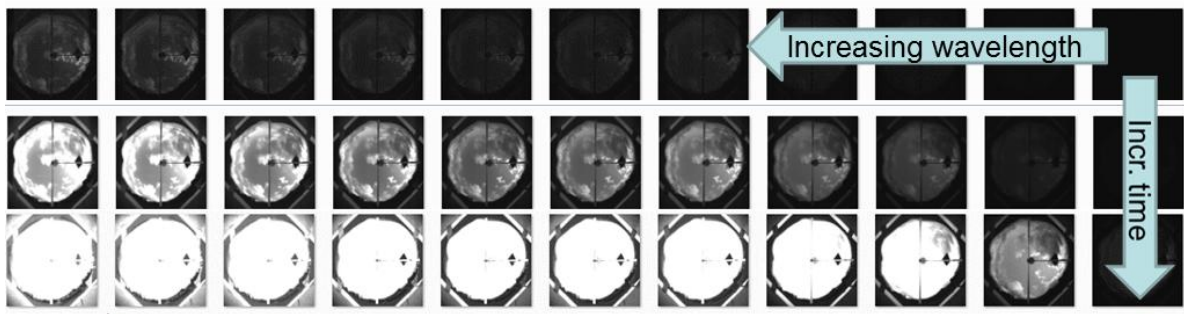


Figure 4. A measurement set made from 33 pictures. Each row is the wavelength series decreasing from left to right from 400 to 300 nm. The exposure time is respectively 1, 10 and 100 ms for the three rows.

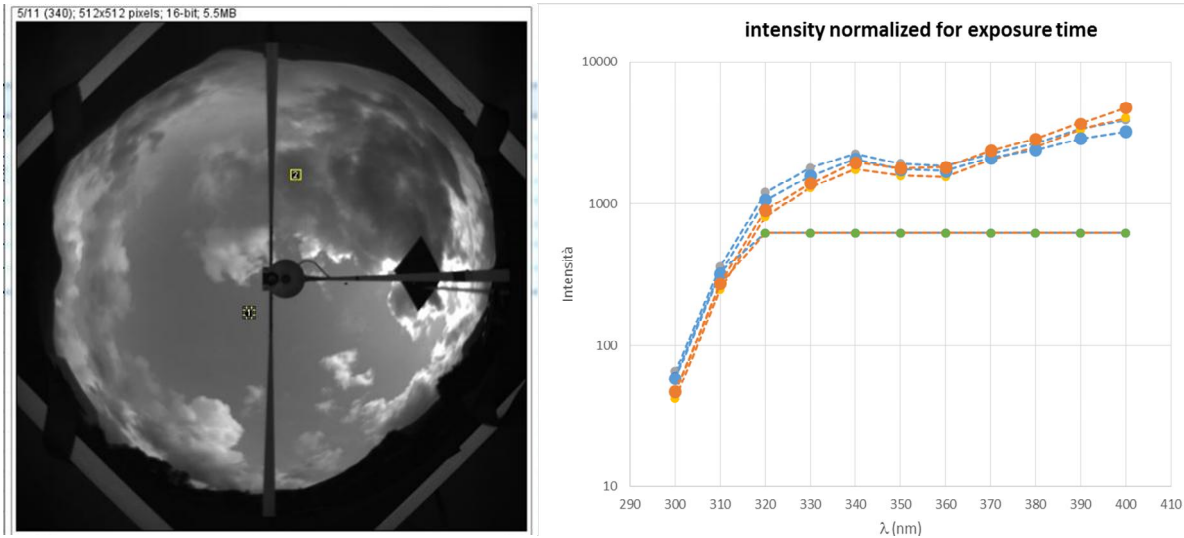


Figure 5. Left: one of the 33 pictures (10 ms 370 nm) where two small portion of the sky are selected. Right: spectral curve for the two points and the three series of pictures normalized for the exposure times. The saturation of the 100 ms exposure series for filters longer than 310 nm is evident.

Specifications and use of MUSKY camera

The instrument has the following specifications:

- Sky coverage: up to 83° Zenith angle
- Spatial resolution: better than 1°
- Spectral resolution: 10 nm
- Spectral range: 300-400 nm in 11 bands
- Overall dimensions: 35x35x70 cm³ (tripod excluded)
- Weight: < 10 kg
- Image output: 512x512 pixel at 16 bit

The MUSKY camera can be easily assembled and dismantled and can be easily transported in a car. A PC is installed close to the instrument and is used to control the motor of the filter wheel and to acquire images from the camera. A second PC is used to remotely control the camera whenever is not convenient to operate close to the instrument.

Conclusions

A multispectral UV wide angle sky camera nicknamed MUSKY has been successfully built and tested. The instrument combines good spatial resolution with an 11 band spectral resolution in the 300 – 400 nm band. The camera is easily transportable and can take spectral images of the whole sky in few seconds. It will be mainly used to develop and validate models used to correct the response of commercial UV radiometers in presence of clouds or other anomalies. A measurement campaign has been carried out in Davos on the 11th, 12th and 16th of July 2014 in presence of clouds and in clear sky conditions. The data will be the basis for the development of the models.

Acknowledgement This work has been supported by the European Metrology Research Programme (EMRP) within the joint research project ENV03 “Traceability for surface spectral solar ultraviolet radiation” (SolarUV). The EMRP is jointly funded by the EMRP participating countries within EURAMET and the European Union.

Using a laser driven light source for spectral responsivity calibration of detectors between 250 and 400 nm wavelengths

Paul R. Dekker* and Omar El Gawhary

VSL Dutch Metrology Institute, Delft, The Netherlands, * pdekker@vsl.nl

In this research, a method is proposed to overcome the wavelength errors induced by misalignment of a laser driven light source (LDLS) to the entrance port of a monochromator-based facility for calibration of spectral responsivity of detectors and filter radiometers.

Source

Xenon arc lamps are often used in combination with a monochromator to provide the spectrally tunable flux needed for calibration of the spectral responsivity of detectors [1,2]. However, the poor short term stability (about 0.2%) of these lamps often dominates the uncertainty budget of the spectral responsivity of detectors, as well as those of filter radiometers calibrated through similar procedure, especially in the UV range of the electromagnetic spectrum. With the aim of reducing the said calibration uncertainty, a Laser-Driven Light Source (LDLS) [3] has been used to power the monochromator-based facility in use at VSL. A photograph of the LDLS fitted with a dual parabolic mirror based focusing optics, mounted on the motorised source translation stage is shown in Fig. 1.



Figure 1. Laser driven light source and focusing optics on the translation stage of the spectral responsivity facility.

Spectrally tunable light sources based on an LDLS, combined with a reflection grating systems, have been studied previously [4,5]. Although the application performances of an LDLS on monochromator-based calibration facility for detector has been studied, the differences and the additional complications with respect to the source alignment, have not yet been properly investigated. As can be expected, due to the small size of the plasma spot (about 100 μm) of the LDLS, alignment to the relatively large entrance slit (2.5 mm) of the

monochromator proved to be critical. Vertical and angular misalignment of the LDLS can cause asymmetry and shifts in the spectral distribution of the flux at the exit slit of the monochromator. Wavelength errors of several nanometers are easily observed when the LDLS is aligned to the entrance of the monochromator by using the common procedures typically used. The slit width of the monochromator was not reduced in size to provide a good signal-to-noise ratio in the wavelength calibration of the monochromator against spectral calibration lamps and to enable a comparison with the measurements performed through the common sources, e.g. Tungsten halogen lamp and Xenon arc. Instead the LDLS has been further aligned based on the spectral distribution at the exit of the monochromator.

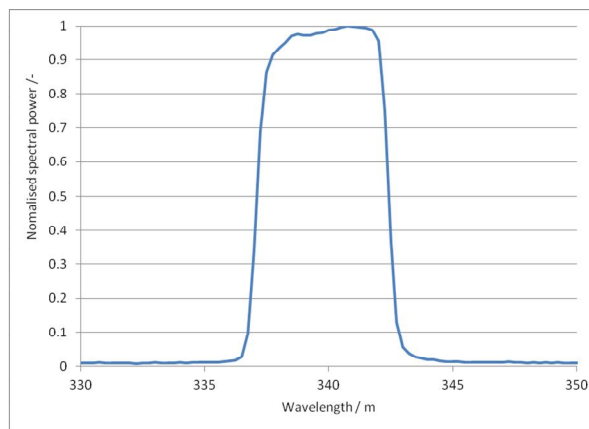


Figure 2. Normalised spectral power of monochromator-based detector calibration facility equipped with laser driven light source measured at a wavelength of 340 nm.

Wavelength based alignment

To measure the spectral distribution of the quasi-monochromatic light used to calibrate spectral responsivity of detectors, the beam exiting the output slit of the monochromator was sent into a 2" diameter integrating sphere and coupled into a fiber based array spectroradiometer. The wavelength scale of the spectroradiometer was independently calibrated against a wavelength ruler recently built at VSL, providing a scale in the spectral range 280 – 400 nm. The vertical alignment of the LDLS was optimized so that the effective wavelength of the spectrum measured would match the wavelength setting of the monochromator. Subsequently, the angular alignment of the LDLS to the entrance port was optimized to get a symmetrical spectral distribution. Figure 2 shows an example of the normalised spectral power of monochromator-based detector calibration facility equipped with laser driven

light source measured at a wavelength of 340 nm after alignment of the LDLS. Following this procedure, the wavelength error due to misalignment of the LDLS has been reduced to 0.09 nm, which is well below the wavelength uncertainty of approximately 0.2 nm. Furthermore, by implementing the LDLS, the uncertainty contribution of source stability on the spectral responsivity calibration could be reduced to only 0.04 %.

Acknowledgements The research presented in this project has been partly funded by EMRP ENV03 project "Traceability for surface spectral solar ultraviolet radiation" (SolarUV). The EMRP is jointly funded by the EMRP participating countries within EURAMET and the European Union. Also, the authors acknowledge partial support from the Ministerie van Economische Zaken, the Netherlands

References

[1] C. A. Schrama, R. Bosma, K. Gibb, H. Reijn, and P. Bloembergen, "Comparison of monochromator-based and laser-based cryogenic radiometry," *Metrologia* **35**, 431–435 (1998).

- [2] P. Meindl, A. E. Klinkmüller, L. Werner, U. Johannsen, and K. Grützmacher, "New UV spectral responsivity scale of the PTB based on a cryogenic radiometer and an argon plasma arc radiation source," *Metrologia* **43**, S72–S77 (2006).
- [3] S. Horne, D. Smith, M. Besen, M. Partlow, D. Stolyarov, H. Zhu, W. Holber, "A novel high-brightness broadband light-source technology from the VUV to the IR," *Proc. SPIE* **7680**, 76800L-1–7 (2010).
- [4] J. Feng, J. Nasiatka, J. Wong, X. Chen, S. Hidalgo, T. Vecchione, H. Zhu, F. J. Palomares, and H. A. Padmore, "A stigmatic ultraviolet-visible monochromator for use with a high brightness laser driven plasma light source," *Rev. Sci. Instrum.* **84**, 085114 (2013).
- [5] U. Arp, R. Vest, J. Houston, and T. Lucatorto, "Argon mini-arc meets its match: use of a laser-driven plasma source in ultraviolet-detector calibrations," *Appl. Opt.* **53**, 1089–1093 (2014).

A Laser-Driven Light Source (LDLS) as a portable spectral irradiance calibration source in the UV range

O. El Gawhary^{1,}, S. A. van den Berg¹, N. van der Leden¹, P. Dekker¹, and M. Khazova²*

1. VSL Dutch Metrology Institute, Delft, The Netherlands, * oelgawhary@vsl.nl
2. Public Health England, Laser and optical radiation dosimetry, United Kingdom

Introduction

An important requirement of any accurate experiment is to be under statistical control. This means that once the aimed uncertainty u (in percent) for the quantity of interest is specified, it has to be guaranteed that the signal to noise ratio (SNR) of the measured quantity stays always roughly larger than $3/u$.

For accurate measurements, this sets quite stringent requirements on the minimum values for the signal to be measured. Calibration measurements do not represent an exception in this sense. For this reason, in many radiometric applications it is highly desirable to have available light sources which show excellent temporal stability and high spectral irradiance, or spectral radiance, depending on the specific application, levels and that, possibly, are still not too complex to be operated in practice.

In this context, in the last few years a new class of laser-driven plasma sources has been made available for the radiometry community. These sources generate a broadband spectrum, with high irradiance levels, particularly appealing in the range 280 – 400 nm which makes them of special interest for calibration of spectroradiometers for measurements of the UV component of solar radiation reaching the Earth.

Within the framework of the EMRP project ENV03, “Traceability for surface spectral solar ultraviolet radiation,” a feasibility study on using a Laser-Driven Light Source (LDLS), by Energetiq, as a spectral irradiance calibration tool has been performed.

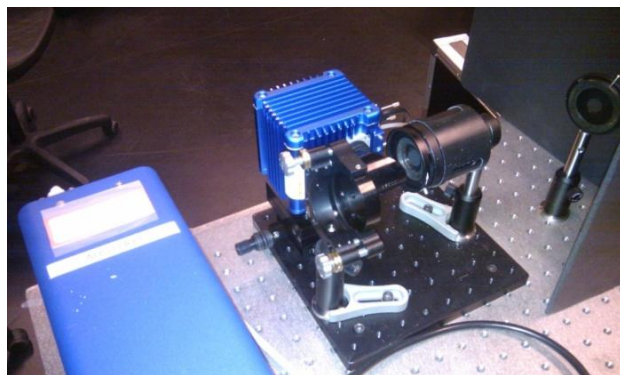


Figure 1. A LDLS source collimated by a 2" focal length off-axis parabolic mirror. A long pass filter, cutting at 280 nm, is also introduced to prevent short wavelength radiation from reaching the spectroradiometer intended to be used to measure the spectral irradiance level.

Collimating the source

The Light Driven Light Source (LDLS) is a broad-band source, characterized by a pretty flat spectral emission, ranging from about 170 nm to 2100 nm. This is appealing, especially for the UV part, since typically in that region of the spectrum current spectral irradiance standards (such as 1000 W halogen lamps) show a large spectral irradiance drop. However, since the plasma source is highly divergent, and the total flux emitted from the source is much smaller than from a FEL lamp, still pretty low spectral irradiance levels (below $0.03 \text{ W m}^{-2} \text{ nm}^{-1}$) at 50 cm distance from the lamp are obtained. Additionally, the large beam divergence makes inaccuracies in distance determination very critical. In order to have higher irradiance levels and remove the tight requirements for the distance determination, we have collimated the light source by using an off-axis parabolic mirror (Fig. 1). Because of the small plasma spot of about $100 \mu\text{m}$, this source is very suitable for collimation. At a distance of 30 cm, this results in high UV spectral irradiance levels, as shown in Fig. 2. We have also performed studies to estimate the beam homogeneity on the x,y plane, an important feature for a spectral irradiance source, along with the sensitivity with respect to z -displacements for such collimated beam.

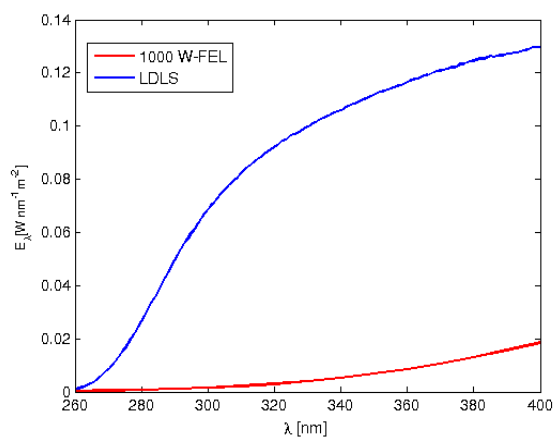


Figure 2. Spectral irradiance of collimated LDLS, at 30 cm distance, (blue line) compared to the spectral irradiance of a 1000 W FEL lamp at 50 cm distance (red line). The spectral irradiance drop below 280 nm for the LDLS is due to the insertion of a long-pass filter included after the mirror, in order to block short wavelength radiation.

The sensitivity coefficients for the three directions, with respect to spatial displacements, resulted to be in the worst case (measured at 280 nm, 340 nm and 400 nm),

$S_x \approx 2 \text{ \%}/\text{mm}$, $S_y \approx 0.5 \text{ \%}/\text{mm}$ and $S_z \approx 0.012 \text{ \%}/\text{mm}$. While the quality of the collimation is very good, the large sensitivity with respect to the x displacement is a matter of concern and ways to improve it should be implemented in the future. We have also observed the beam inhomogeneity by means of a beam profiler in a region of about 11 mm diameter around the center of the beam, which essentially confirms the spectral irradiance measurements (Fig.3). In Fig. 4 we also show two different spectral irradiance curves of the LDLS, measured at 30 cm and 50 cm, respectively, just to point out the little difference in spectral irradiance values even for such a large distance variation.

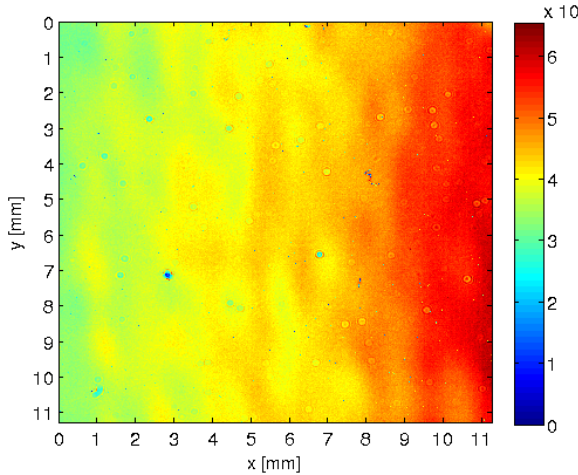


Figure 3. Intensity distribution of the collimated LDLS across a x,y plane.

Determination of an array spectroradiometer response

The LDLS has been used to determine the spectral irradiance responsivity of an array spectroradiometer, as compared to the responsivity obtained through a standard 1000 W FEL lamp. The array spectrometer is a QE65000, which an Ocean Optics array spectrometer with 230 – 410 nm spectral range, 50 μm slit, cooled, with a 2" averaging sphere as entrance optics consists, half/inch input port, fiber coupled. A general description of the device and its performances are available in [1, 2].

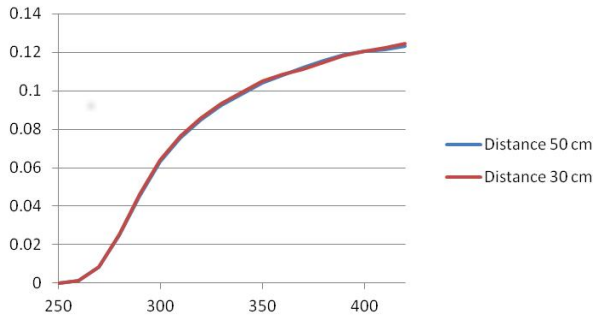


Figure 4. Spectral irradiance change due to distance variation.

The agreement between the two responsivities is within 2 % above 340 nm and it drops around 330 nm between 4 % and 6 %. A deviation of 2 % is within the combined uncertainty of the spectral irradiance of the two light

sources. The larger deviation around 300 nm has to be further investigated. Possible reasons at the origin of it could be reproducibility problems or residual straylight corrections issues, considered that the spectral irradiances of the two light sources are very different, being flat for the LDLS while the 1000 W FEL lamp has a large infrared contribution and a very poor one in the UV part of the spectrum.

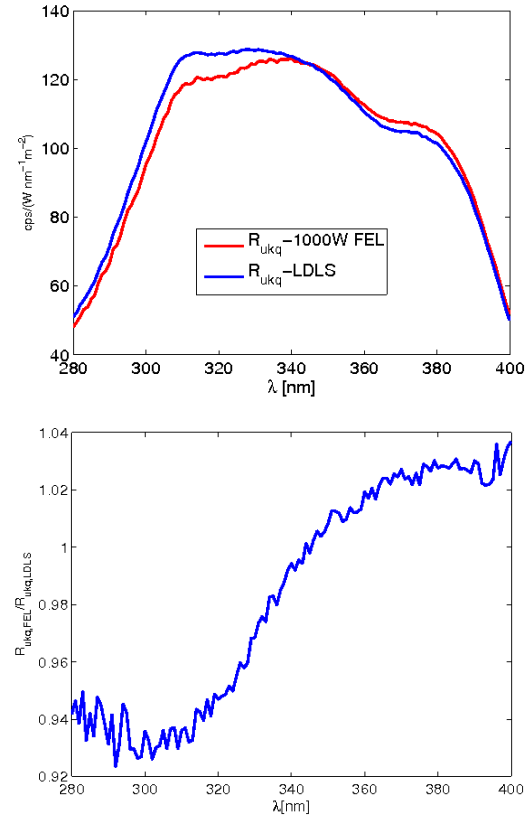


Figure 5. a) Responsivity, as $\text{cps}/(\text{W m}^{-2} \text{ nm}^{-1})$ as obtained by means of a 1000 W FEL lamp (red line) and LDLS (blue line). b) ratio of the two obtained responses.

Conclusions

The possibility of using a Light Driven Light Source (LDLS) as spectral irradiance source for calibration of spectroradiometers operating in the UV part of the spectrum has been discussed. After collimation, the source shows spectral irradiance levels at least one order of magnitude higher than a 1000 W FEL lamp which, along with a good temporal stability, makes the source appealing for spectral irradiance responsivity characterization of spectroradiometer in the UV part of the electromagnetic spectrum. Additionally, the requirements of accurately determining the reference plane of the instrument under consideration are strongly relaxed. On the other hand, the quality and homogeneity of the collimated beam needs to be improved. Despite this, the first results on the calibration of the responsivity of spectroradiometers are very promising.

Thematic Network for Ultraviolet Measurements

Acknowledgement This work has been supported by the European Metrology Research Programme (EMRP) within the joint research project ENV03 “Traceability for surface spectral solar ultraviolet radiation” (SolarUV). The EMRP is jointly funded by the EMRP participating countries within EURAMET and the European Union.

References

[1] L. Price, R. Hooke, and M. Khazova, “Temperature dependence of array spectroradiometers and implications

for photobiologists,” *Proc. CIE 2014 Lighting Quality & Energy Efficiency*, CIE x039:2014, 950-956 (2014).

[2] L. A. Price, R. J. Hooke, and M. Khazova, “Effects of ambient temperature on performance of CCD array spectroradiometers and practical implications for field measurements,” *J. Radiol. Prot.* (in press).

Improved diffusers for spectroradiometers measuring solar irradiance

Petri Kärhä^{1,2}, Joop Mes³, Tomi Pulli¹, Josef Schreder⁴, Allard Partosoebroto³, Gregor Hülsen⁵, Janne Askola¹, and Julian Gröbner⁵

1. Aalto University, Espoo, Finland
2. Centre for Metrology and Accreditation MIKES, Espoo, Finland
3. Kipp & Zonen, Delft, The Netherlands
4. CMS - Ing. Dr. Schreder GmbH, Kirchbichl, Austria
5. Physikalisch-Meteorologisches Observatorium Davos, World Radiation Center, Davos, Switzerland

Introduction

In the project EMRP ENV03 “Traceability for surface solar UV measurements,” we have developed software based on Monte Carlo analysis that can be used to simulate cosine responses of diffusers used in solar UV measurements [1,2]. The software can be used in assisting development work of new diffuser types, as has been described in [3].

The simulation algorithm assumes the topology of Fig. 1 for the diffuser assembly. Any of the parameters shown can be varied to tailor the properties of the diffuser. The parts of the diffuser assembly include 1. the actual diffuser element, 2. the housing used to attach the element to the detector / fiber, 3. a shadow ring blocking light at large zenith angles, 4. a protective quartz dome, and 5. the detector / fiber detecting the photons that pass through the assembly.

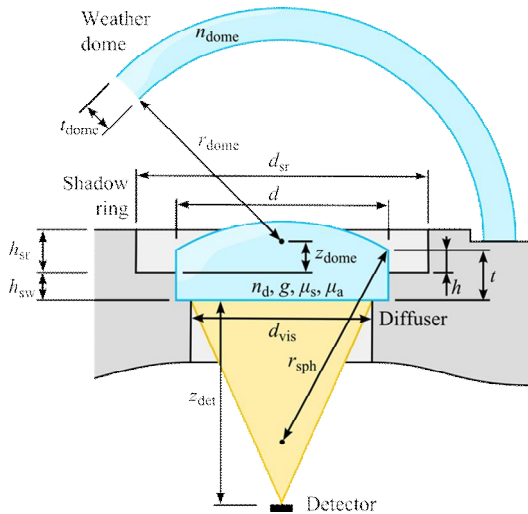


Figure 1. Structure of a diffuser showing parameters that can be varied, when optimizing the cosine response of the input optics.

The software was used in assisting the development work of two types of diffuser assemblies, 1. an assembly to replace the standard diffuser assembly of Brewer spectroradiometers (developed by Kipp & Zonen), and 2. an assembly to be coupled into fibers or fiber bundles used with certain types of spectroradiometers (developed by CMS Schreder GmbH).

The work started with finding suitable material to be used as the diffuser element. Prototype diffusers were assembled with various PTFE materials and novel Quartz

samples [4] and measured for their transmissive and angular properties. Comparison of the material properties, plotted as transmission vs. cosine error, can be seen in Fig. 2. The closer the sample is to the upper left corner, the more ideal the material is as a diffuser.

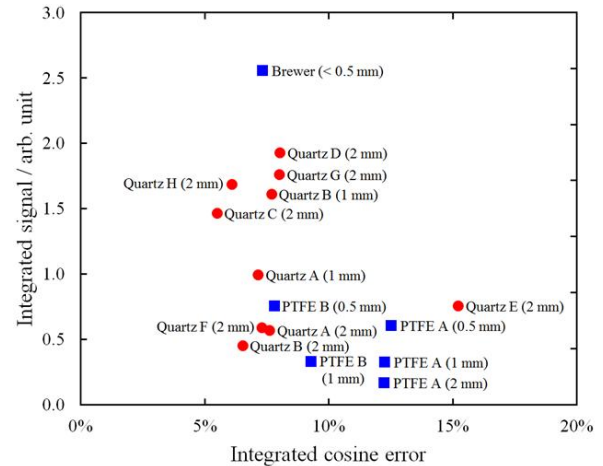


Figure 2. Transmissive and angular properties of the materials studied. Quartz samples are indicated with red circles, PTFE materials with blue squares. An ideal diffuser (material) would occupy the upper left corner.

Based on the measurements, Quartz material H was selected to be used in the diffusers. The material is Quartz with small gas bubbles blown into the material during the manufacturing process. Both sides of the elements are polished. Samples with thicknesses between 1 – 2 mm were tested. The final properties and some details of the development work are described in this article.

New diffuser for Brewer spectroradiometers

The new diffuser developed by Kipp & Zonen to be used with Brewer spectroradiometers, utilizes a flat quartz diffuser, 22 mm in diameter. The diffuser has a weather dome. A photograph of the diffuser assembled on a Brewer Mark III spectroradiometer is presented in Fig. 3 a). Figure 3 b) shows the simulated and measured cosine errors for the prototype of the new diffuser.

The Brewer spectroradiometer can measure both direct and global UV radiation. The original global UV port has a PTFE diffuser which has an integrated cosine error of $f_2 = 5\%$. Combined with the non-ideal properties of PTFE such as aging and temperature dependent transmission, the diffuser causes a significant uncertainty

Thematic Network for Ultraviolet Measurements

in the UV measurements. The newly developed prototype diffuser is based on a 2 mm thick, flat sintered quartz disk. It is mounted onto an adjustable tube connected to the fore-optics of the instrument, as opposed to the original diffuser which is built into the weather cover of the instrument.



Figure 3. a) Photograph of the new Brewer diffuser b) Measured (symbols) and simulated (lines) cosine errors for the new diffuser.

New diffuser for spectroradiometers with fiber connection

The new diffuser developed by CMS Schreder to be used with fiber coupled spectroradiometers, utilizes a flat quartz diffuser, 11 mm in diameter. The diffuser has a removable weather dome. The assembly can be fitted to various fibers including e.g. a single mode optical fiber with an SMA connector or a fiber bundle. A photograph of the diffuser is presented in Fig. 4 a).



Figure 4. a) Photograph of the new fiber coupled Schreder diffuser b) Measured (symbols) and simulated (lines) cosine errors for the new fiber diffuser. The effect of the quartz dome can be clearly seen by comparing the results with and without the dome.

The final diffuser assembly was measured for azimuthal response. The maximum variation in the responsivity was $\pm 1.5\%$ when rotated over 360° around optical axis and looking at a source at the zenith angle of 70° . The diffuser offset [5] was measured to be 0.3 mm in the visible region. In the UV region, it should be smaller.

Conclusions

A Monte Carlo based algorithm for simulating diffusers was developed. The algorithm accounts for the diffuser element itself as well as the surrounding elements, such

Several iterations between simulated and measured responses have led to a good agreement between the simulations and the observed directional responses. The transmission of the new design is approximately 20 % lower than the original diffuser, but a much improved directional response, integrated cosine error of $f_2 = 1.3\%$, is obtained. The new diffuser is to be supplied by Kipp & Zonen.

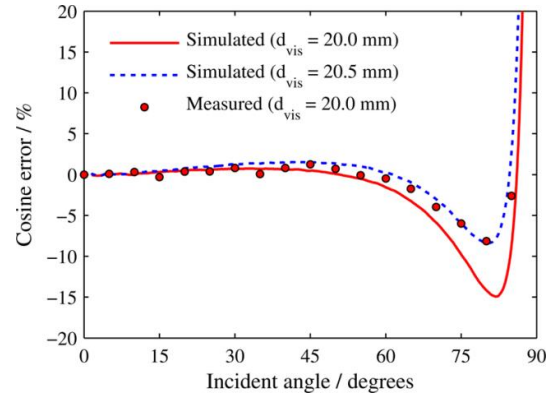
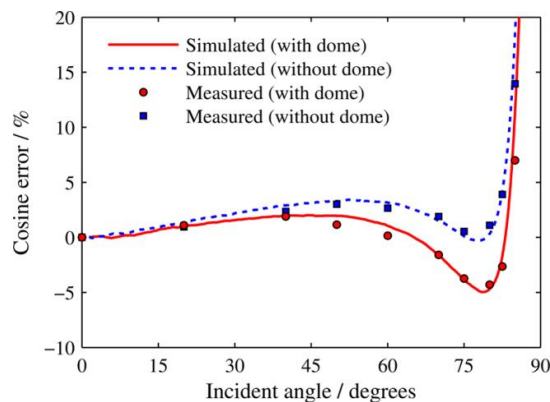


Figure 4 b) shows simulated and measured cosine errors for the prototype of the new diffuser. The integrated cosine error $f_2 = 1.4\%$. The simulation results agree quite well into the measurements. However, a small correction in the parameters had to be made. The angular response of the fiber was not measured, thus the diameter of the area of the back wall of the diffuser element seen by the field-of-view of the fiber end had to be slightly adjusted.



as the shadow ring and the weather dome of the entrance optics.

The algorithm was used to guide the design process of two diffuser assemblies, a fiber coupled diffuser and a diffuser for the Brewer spectroradiometer, constructed by CMS Schreder GmbH and Kipp & Zonen, respectively. Both entrance optics designs utilized novel quartz-based diffuser elements with gas bubbles blown into the material to act as scattering centers. These diffuser elements have variety of advantageous features as

compared to the more traditional PTFE diffusers, including high transmittance, lack of the sudden phase transition [6] at temperatures around 19 °C, and better stability. The measured integrated cosine errors f_2 of the fiber coupled and Brewer diffusers were 1.4 % and 1.3 %, respectively.

Acknowledgement This work has been supported by the European Metrology Research Programme (EMRP) within the joint research project ENV03 “Traceability for surface spectral solar ultraviolet radiation” (SolarUV). The EMRP is jointly funded by the EMRP participating countries within EURAMET and the European Union.

References

[1] T. Pulli, P. Kärhä, J. Mes, and J. Schreder, “Software for designing solar UV diffusers,” *UVNews* **9**, 7–9 (2013).

[2] T. Pulli, P. Kärhä, and E. Ikonen, “A method for optimizing the cosine response of solar UV diffusers,” *J. Geophys. Res. Atmos.* **118**, 7897–7904 (2013).

[3] T. Pulli, “Improved Diffusers for Solar UV Spectroradiometers,” *Thesis for the degree of M.Sc. in technology*, 9 + 48 pp., Aalto University, Espoo (2013).

[4] B. Barton, P. Sperfeld, S. Nowy, A. Towara, A. Höpe, S. Teichert, G. Hopfenmüller, M. Baer, and T. Kreuzberger, “Characterization of new optical diffusers used in high irradiance UV radiometers,” *Poster presented at NEWRAD 2011*, Maui, Hawaii (2011).

[5] P. Manninen, J. Hovila, L. Seppälä, P. Kärhä, L. Ylianttila, and E. Ikonen, “Determination of distance offsets of diffusers for accurate radiometric measurements,” *Metrologia* **43**, S120 (2006).

[6] L. Ylianttila and J. Schreder, “Temperature effects of PTFE diffusers,” *Opt. Mater.* **27**, 1811–1814 (2005).

Devices for characterizing the wavelength scale of UV spectrometers

Peter Blattner^{1,*}, Stella M. Foaleng¹, Steven van den Berg², Omar El Gawhary²,
M. Blumthaler³, Julian Gröbner⁴, and Luca Egli⁴

1. Federal Institute of Metrology, Bern-Wabern, Switzerland, * peter.blattner@metas.ch
2. VSL Dutch Metrology Institute, Delft, The Netherlands
3. Innsbruck Medical University, Biomedical Physics, Innsbruck, Austria
4. Physikalisches-Meteorologisches Observatorium Davos, World Radiation Center, Davos, Switzerland

Accurate wavelength calibration is a key parameter for solar spectral measurements. Typically, spectroradiometers are calibrated with spectral emission lines. However, for small spectral ranges only few lines are typically available. Within the framework of an EMRP Project solarUV, novel devices for wavelength calibration were realized.

Introduction

For the measurement of solar UV radiation that reaches the earth, there is a need for improved accuracy of the wavelength scale. Due to absorption by ozone for wavelengths below 330 nm, a large dynamic range is required for measuring spectral irradiance throughout the solar UV wavelength range (280 – 400 nm). This also puts stringent requirements on the accuracy of the wavelength scale, since a small difference in wavelength implies a large difference in spectral irradiance, when measuring close to the edge of the ozone absorption. For this reason, wavelength uncertainties below 50 pm are needed.

Typically, spectrometers are calibrated with spectral emission lines from e.g. Hg-lamps. However, for small spectral ranges only few lines are typically available. In addition, some of the spectral lines are caused by multiplets (e.g. Hg-lines at 313 nm, 365 nm, 404 nm and 408 nm), or may have very low levels (297 nm, 302 nm and 334 nm) and cannot be used by typical solar UV spectrometers. Often only two spectral lines are available at 253.6521 nm and 435.8335 nm (see Fig. 1).

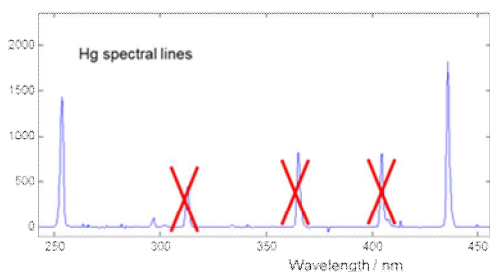


Figure 1. Spectral emission lines of a Hg calibration lamp.

Within the EMRP project solarUV, different devices were realized that allow characterizing the wavelength scale accurately all over the UV (and visible) spectral range: METAS realized devices based on different Fabry-Perot etalons. VSL developed a wavelength ruler that is based on a one-stage Lyot filter. These devices show an oscillating transmittance behaviour that can theoretically

be modelled knowing the optical thicknesses of the device (see Figs. 2 and 3).

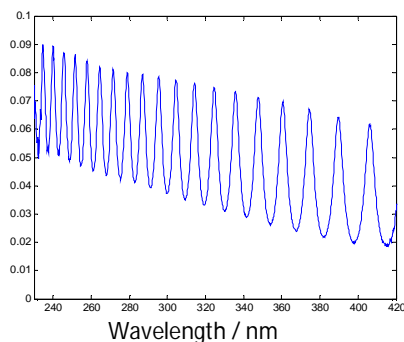


Figure 2. Spectral transmittance of a Fabry Perot etalon.

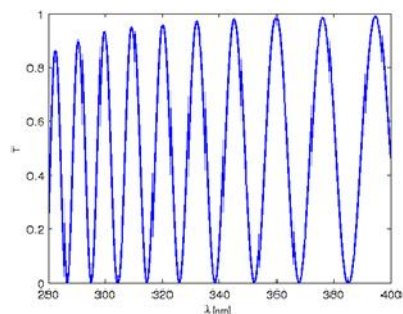


Figure 3. Spectral transmittance of one-stage Lyot filter.

The devices can be used with any kind of “white” light sources, but for best performance (i.e. to generate stable and powerful radiation in the UV range) a laser driven light source is recommended to be used. In the first step, the transmittance is experimentally determined by measuring the spectral distribution of the light source with and without the filter. This transmittance is then compared to the theoretically modelled transmittance. If the optical thicknesses of the device are not known, or the setup does not respect the conditions for absolute devices, it is possible to use the device in combination with known spectral lines of a mercury lamp or one or several lasers. In this case, an optimization algorithm has to be used to retrieve the effective optical thicknesses.

Fabry-Perot etalon devices

Initial work on Fabry-Perot etalon has been presented by Balmer and Heuberger [1] using a Fabry-Perot etalon based on Mica. Unfortunately Mica has a high

absorbance in the UV region. In the frame work of the EMRP-project ENV03, different Fabry-Perot etalons were realized and characterized with respect to temperature, uniformity, and angular dependence. The Fabry-Perot is based on a thin layer of fused silica coated on both sides by semi-transparent mirrors. For this purpose a 525 μm thick SiO_2 (silica) substrate was used as support. The first mirror was created by sputtering a 10 nm thick Al layer on one side of the substrate. At the next step, a 3 μm to 9 μm thick fused silica layer was created using a Low Pressure Chemical Vapor Deposition at Low Temperature Oxide (LPCVD-LTO) process. The second Al mirror was deposited with a thickness of 10 nm using sputtering process. Figure 2 shows the measured transmittance of a Fabry-Perot etalon with a SiO_2 of 3.1 μm thickness.

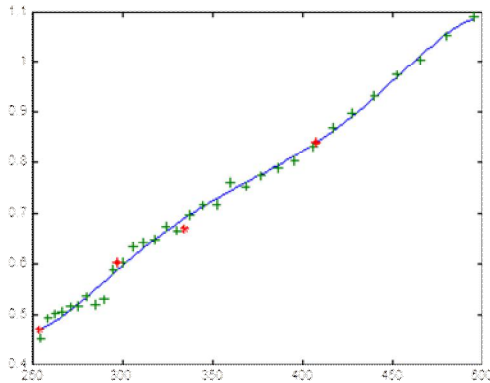


Figure 4. Measured wavelength error (in nm) as a function of the wavelength (nm) prior to correction.

The optical transmittance can be characterized by using a multi-layer thin film model. Basically the refractive indices of the layers are given in the literature. The optical thicknesses of the SiO_2 and Al layers are free parameters that have to be optimized in order to fit the model to the measured values.

The device can reduce the uncertainty of the wavelength scale to well below 50 pm. Figure 4 shows the error of the wavelength scale of a particular spectrometer obtained by a Fabry-Perot device. The red crosses indicate the errors obtained by a Hg lamp calibration.

After correction, the error reduces to within ± 20 pm (Figure 5). If the temperature conditions are controlled (typically to better than 2 $^\circ\text{C}$) and the geometry is fixed (angular alignment and beam divergence better than 0.5°) the devices can be used as absolute devices, and deviations of the wavelength scale can be directly identified.

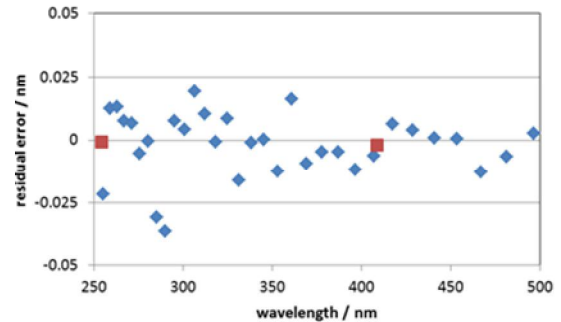


Figure 5. Residual error after wavelength correction.

Conclusions

The performance of the device has been successfully demonstrated during an international comparison of UV spectrometers at PMOD/WRC Davos in July 2014. Several spectrometers were characterized and the wavelength errors of these devices could be reduced to below 50 pm. The Fabry Perot etalon is a very compact optical element which can be easily integrated into an instrument.

Acknowledgement This work has been supported by the European Metrology Research Programme (EMRP) within the joint research project ENV03 “Traceability for surface spectral solar ultraviolet radiation” (SolarUV). The EMRP is jointly funded by the EMRP participating countries within EURAMET and the European Union.

Reference

- [1] Peter Blattner, Stella M. Foaleng, Steven van den Berg, Omar El Gawhary, M. Blumthaler, Julian Gröbner, and Luca Egli, “Devices for characterizing the wavelength scale of UV spectrometers,” *Proceedings of the Newrad 2014*, pp. 201–202 (2014).

Regular articles

The GUVis-3511: a new multi-channel radiometer for monitoring UV and visible radiation

Germar Bernhard, Randall N. Lind, James C. Ebrahimian, and Charles R. Booth

Biospherical Instruments, San Diego, USA

Biospherical Instruments Inc. (BSI) has released a new multi-channel radiometer for monitoring UV and visible radiation, the GUVis-3511 (Fig. 1). The instrument is the successor of the widely used GUV-511 and GUV-2511 ground-based ultraviolet (UV) monitoring instruments, which are deployed world-wide in UV monitoring networks. While the GUV-2511 was limited to a maximum of seven channels, the GUVis-3511 is available with as many as 19 channels, which can be selected from over 30 wavelengths, ranging between 305 and 1,640 nm. The radiometer can also measure Photosynthetically Available Radiation (PAR; 400-700 nm). The instrument uses specialized, hard-coat, multicavity interference filters with excellent long-term stability. It is environmentally sealed and temperature-stabilized, designed for long-term operation in harsh environments. The instrument is controlled via proprietary data acquisition software running under Windows® operating systems.

The GUVis-3511's electronics have been completely redesigned from its predecessors. They are now based on BSI's microradiometer technology, which features unprecedented performance with respect to dynamic range, linearity, speed, and expandability. The instrument also features a newly-designed irradiance collector with a small cosine error from the UV to the infrared (Fig. 2).

A shadowband accessory is also available, which allows alternating measurements of global (sun + sky) and diffuse solar irradiance. These measurements allow the calculation of direct solar irradiance and related data products such as aerosol optical depth. The accessory is suitable both for deployments on stationary and moving platforms, including ships, where the position of the Sun is not defined. A fully integrated Global Positioning System (GPS) is also available. One instrument has recently been successfully deployed on a research vessel transecting the Atlantic Ocean from South to North.

The instrument is based on technology developed under the project "Optical Sensors for Planetary Radiant Energy" (OSPRey). OSPRey was a joint project between BSI and NASA to develop a state-of-the-art above-water radiometer system in support of current and next-generation ocean color satellite missions [1].



Figure 1. GUVis-3511 radiometer (center) with shadowband and GPS accessories.

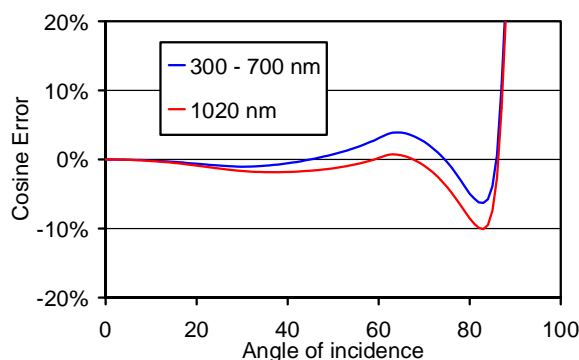


Figure 2. Cosine error of a GUVis-3511 radiometer. The newly-designed irradiance collector features low cosine errors from the UV to the infrared.

Additional information, including a comprehensive list of specifications, is available at www.biospherical.com.

References

- [1] S.B. Hooker, G. Bernhard, J.H. Morrow, C.R. Booth, T. Comer, R.N. Lind, and V. Quang, *Optical Sensors for Planetary Radiant Energy (OSPRey): Calibration and Validation of Current and Next-Generation NASA Missions*, NASA Tech. Memo. 215872, NASA Goddard Space Flight Center, Greenbelt, Maryland (2012). Available at:

<http://www.biospherical.com/images/pdf/hooker-215872-rs.pdf>

Characterization of UV photodiodes in the ultraviolet spectral region

*Luciana C. Alves**, *Thiago Menegotto*, *Thiago Ferreira da Silva*, *Jaqueline S. P. M. Corrêa*, and *Iasmim F. Duarte*

National Institute of Metrology, Quality and Technology – Inmetro, Duque de Caxias, Brazil

* *lcalves-pronametro@inmetro.gov.br*

UV-100L, GaAsP and PtSi-n-Si UV photodiodes have been characterized in spectral power responsivity and shunt resistance. The local responsivity characteristic function has also been studied for UV-100L photodiodes. The results are used in the selection of photodiodes for constructing UV radiometers to be used as transfer standards in the metrology traceability chain.

Introduction

The transfer of the radiometric scale of absolute spectral power responsivity from the cryogenic radiometer has been traditionally performed by reflection trap detectors with three silicon photodiodes. In the visible (VIS) and near infrared (NIR) spectral regions, Hamamatsu S1337 silicon photodiode has been usually chosen for the construction of these trap detectors. However, in the ultraviolet (UV) spectral region this type of photodiode is not appropriate since it is difficult to interpolate the quantum efficiency below 400 nm [1]. Additionally, the spectral power responsivity of S1337 photodiodes can be affected by exposure to ultraviolet radiation [2-4]. These limitations are overcome with the use of a suitable kind of photodiode, such as Schottky barrier photodiodes [2-4].

In this study, we investigated the spectral power responsivity and shunt resistance of UDT UV-100L UV-enhanced silicon (inversion layer) photodiodes, Hamamatsu G2119 GaAsP Schottky photodiodes and SUV-Detectors PtSi-n-Si Schottky photodiodes. The local responsivity characteristic function has also been studied in case of the UV-100L photodiode.

Characterization of UV photodiodes

Spectral power responsivity

In this study, two photodiodes of each type were measured using the spectral power responsivity measurement facility of Inmetro. The experimental set-up uses a xenon arc lamp (UV) of 450 W as source of optical radiation. The arc of this lamp is imaged on the entrance slit of a single-grating monochromator, Czerny-Turner type, having 250 mm focal length and 1200 grooves/mm holographic grating. The wavelength scale of the monochromator was calibrated using spectral lamps. Colored glass filters are used to suppress higher-order diffraction. UV-enhanced optical elements were used in order to optimize the radiant power in the system. The entrance and exit slits of the monochromator were adjusted to a width of 1 mm, which corresponds to a bandpass equal to 3 nm. The measurement was performed in the power mode with the photodiode underfilled by the optical beam. The rectangular cross-section of the incident beam is 6 mm high per 1 mm wide. The spectral power responsivity was determined by

extrapolation using an electrically-calibrated pyroelectric radiometer (ECPR) (from Laser Probe Inc.). The ECPR was calibrated to a relative expanded uncertainty of 2.3×10^{-2} ($k = 2$), traceable to the cryogenic radiometer. For spectral responsivity measurements both photodetectors, the UV photodiode under test and the transfer standard detector, were mounted on the same optical rail with a computer-controlled translation stage. Both detectors were covered by a light-tight enclosure and all the measurements were carried out under dark environment conditions. The photocurrent generated at the UV photodiode under test is amplified with a calibrated Vinculum SP042 current to voltage converter, and a Hewlett Packard 34401A digital multimeter is used to measure the voltage. The trans-impedance amplifier gain used for the test detector is typically 10^6 V/A.

Shunt resistance

The shunt resistance of the UV photodiodes (R_{sh}) was determined from the measurement of dark current (I_d) generated for different reverse bias voltage (V_{bias}) values. The $I_d \times V_{bias}$ curves were measured using a HP 4145A semiconductor parameter analyzer and the R_{sh} corresponds to the slope at the origin of the curve.

Local responsivity (spatial uniformity)

The local responsivity characteristic function of the UV-100L photodiodes was measured by spatially scanning its surface within its nominal active area of 1.0 cm^2 using a monochromatic beam (at 350 nm) with small cross-section. The monochromatic beam diameter was limited to 1.0 mm at the plane of the photodiode surface. The spatial uniformity of the photodiodes was investigated by scanning its active area relative to the optical beam over a $12 \times 12 \text{ mm}^2$ area with 0.5 mm steps. All photodiodes were used in the photovoltaic mode (unbiased). A monitor detector and a beam splitter are used behind the monochromator to compensate for drifts in the radiant flux of the optical source.

Experimental results

Figure 1 a) shows the measured spectral power responsivity of the UV photodiodes. The UV photodiodes were calibrated to a relative expanded uncertainty lower than 2.4×10^{-2} ($k = 2$), varying with the wavelength.

The results for the GaAsP photodiodes confirmed its *solar blindness* behavior, with cut-off wavelength around 610 nm, which reduces the infrared stray light for UV filter radiometer application. This type of photodiode has a window made of quartz glass. As expected, PtSi-n-Si Schottky photodiodes are not *solar blind*, as shown in Fig. 1 b), but their spectral responsivity is relatively smooth and flat in the UV spectral region. One UV-100L detector (PT060) presents a hazy surface caused by dust,

which could not be removed by gently cleaning. This can explain the lower responsivity compared to PT062.

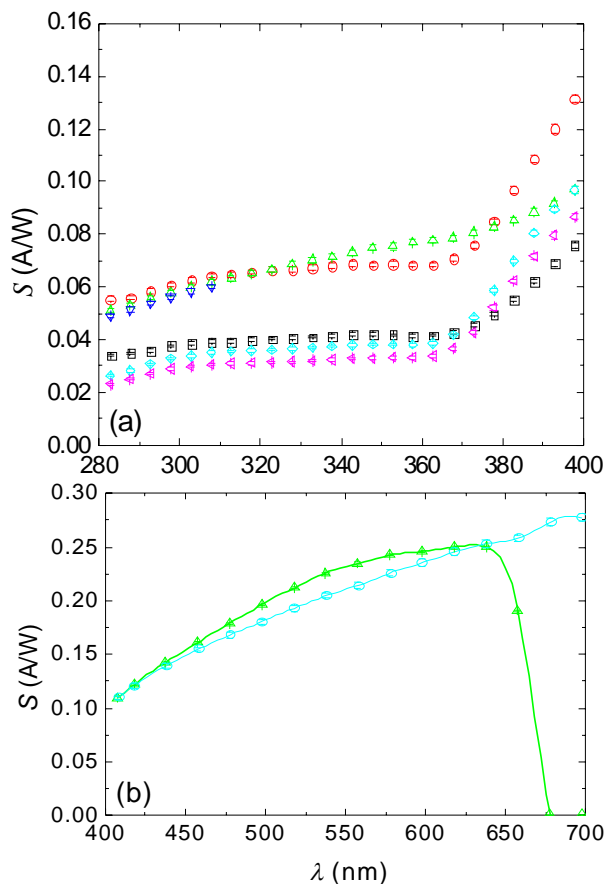


Figure 1. Measured spectral power responsivities of the UV photodiodes: \square UV-100L PT060, \circ UV-100L PT062, Δ G2119-01, \times G2119-03, \diamond PtSi-nSi-01 and \circ PtSi-nSi-02.

The obtained values of R_{sh} are shown in Table 1. The measured R_{sh} of each UV-100L and GaAsP photodiodes is in accordance with the manufacturer values of minimum and typical shunt resistance [5,6]. No literature reference value was found for the PtSi-n-Si Schottky photodiodes.

Table 1. Measured values of shunt resistance R_{sh} of the UV photodiodes.

UV Photodiode	R_{sh} [M Ω]
UV-100L PT060	58.4
UV-100L PT062	42.8
PtSi-n-Si #01	1.3
PtSi-n-Si #02	1.6
G2119 #01	536
G2119 #02	312

The measured local responsivity of the UV-100L photodiodes are shown in Fig. 2.

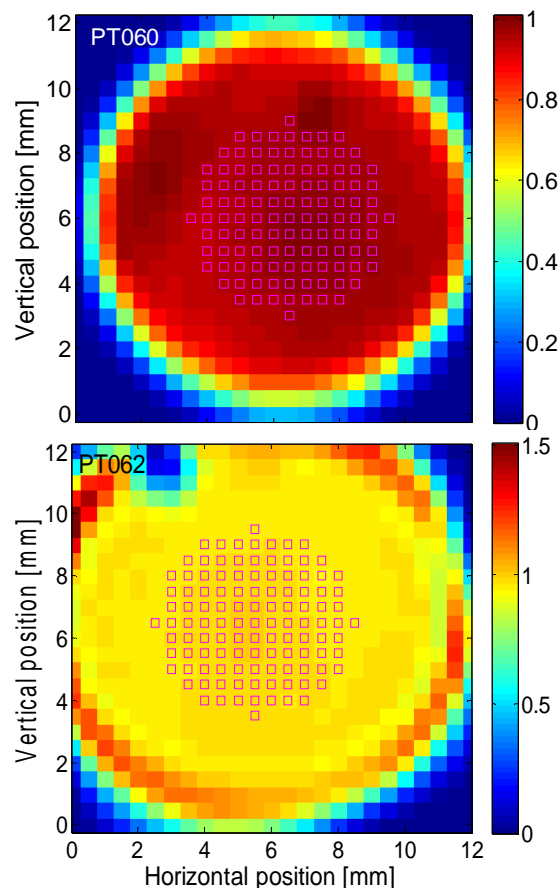


Figure 2. Spatial non-uniformity measured at 350 nm for the UV-100L photodiodes a) PT060 and b) PT062. The squares indicate the region considered in the analysis.

The average spatial non-uniformities of the photodiodes PT060 and PT062 are 0.17 % and 0.26 %, respectively. The values are referenced to the centre of the region corresponding to 50 % of the central active area (indicated by the squares in the figure). An average non-uniformity value smaller than 1.0 % over the active area or smaller than 0.5 % within the 50 % center of the active area is used as a selection criterion. By these parameters, both characterized photodiodes are considered suitable as a transfer standard.

Conclusion

Measurements were realized in order to characterize and select UV photodiodes for being used in the construction of radiometric standard detectors. The next step is to investigate some others characteristics functions of these UV photodiodes prior to use in radiometric measurements, as the local responsivity characteristic function of the Schottky barrier photodiodes. Up to the moment, we found that the G2119 can be a very interesting choice for constructing UVA filter radiometers because of the suppression of radiation above 650 nm and the high shunt resistance.

Acknowledgements L. C. Alves acknowledges the financial support from PRONAMETRO. J. S. P. M. Corrêa and I. F. Duarte acknowledge the support from PROMETRO/CNPq. Authors acknowledge the collaboration of Álvaro Bernardino from Labsem/PUC-Rio in the semiconductor analyzer operation.

References

[1] N. M. Durant and N. P. Fox, "Evaluation of solid-state detectors for ultraviolet radiometric applications," *Metrologia* **32**, 505–508 (1995).

[2] H. Rabus, "For high-accuracy UV detection, PtSi/n-Si Schottky photodiodes offer many advantages," *Oemagazine, SPIE Newsroom* (2003).

[3] K. Solt, H. Melchior, U. Kroth, P. Kuschnerus, V. Persch, H. Rabus, M. Richter, and G. Ulm, "PtSi-n-Si Schottky-barrier photodetectors with stable spectral responsivity in the 120-250 nm spectral range," *Appl. Phys. Lett.* **69**, 3662–3664 (1996).

[4] K. Solt, ETH Zürich, "PtSi-n-Silicon Schottky Barrier Photodiodes for the Ultraviolet and Soft X-Ray Range," (2002).

[5] <http://www.udt.com/>

[6] <http://www.hamamatsu.com/>

The J1006 total sky camera for fast and accurate cloud detection

Josef Schreder

CMS - Ing. Dr. Schreder GmbH, Kirchbichl, Austria

The Total Sky Camera consists of a digital colour camera with up to 4 megapixel resolution. The high-quality lens system with $2\pi / 180^\circ$ field of view is protected by a glass dome and a weather-proof housing, as seen in Fig. 1. It includes the convenience of low power consumption (3W), integrated leveling feeds, dry cartridge system, internal memory (which allows also standalone operation) and a preview mode where the assembly gives instant feedback on instrument orientation. The Total Sky Camera can easily be connected to a computer network through its standard Ethernet interface.

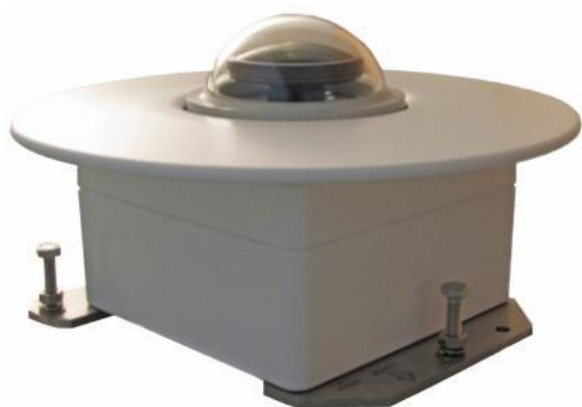


Figure 1. The Total Sky Camera is a fully automatic imaging system capturing pictures of the total, hemispheric sky, which represents the next generation for atmospheric science and solar energy professionals doing site evaluation, monitoring and forecasting.

Sky images are captured either with automated exposure times or with manually defined settings. In autoexposure operation, the pictures are combined into a HDR (high dynamic range) image. This unique method allows an analysis of the sky condition and the cloudiness under full sun illumination conditions without the need for a shading device. Researchers can configure the system and the cloud detection software to their individual requirements.

Through its sophisticated cloud detection algorithm (Fig. 2) and horizon definition tools, the Total Sky Camera can be used as a research tool for weather and cloud observations, grid power management, evaluation of PV performance and solar power forecasting purposes.

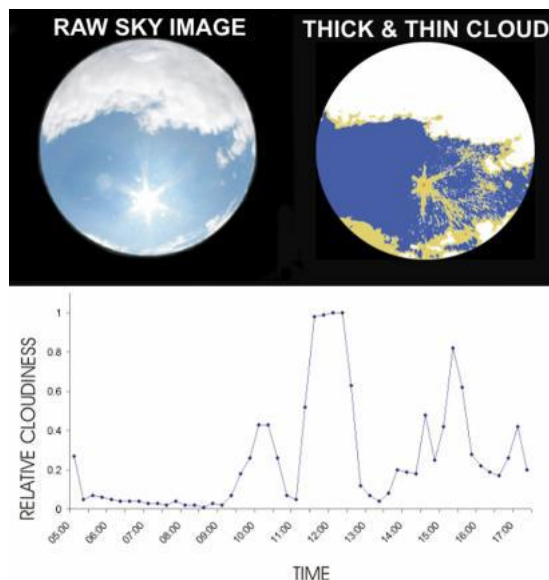


Figure 2. Measurement of the cloud covered sky and the corresponding data analysis showing thick and thin clouds including the variation over the day.

The image processing software automatically calculates the cloud cover fraction. Evaluations of the total sky pictures by the analysis software may be done online on automatic mode or afterwards for campaign based data sets. The software allows classifying the clear sky, the total hemispheric cloud cover, optically thick and thin clouds, the cloud cover of the free horizon or the cloud cover above an artificial horizon.

If the natural horizon is not yet known, the software calculates it by drag-and-drop. In addition the presence of the direct sun is detected. All analysed data are stored as ASCII data including pictures for additional investigations.

References

1. J. M. Sabburg and C.N. Long, "Improved sky imaging for studies of enhanced UV irradiance," *Atmos. Chem. Phys. Discuss.* **4**, 6213–6238 (2004).
2. A. Kreuter, M. Zangerl, M. Schwarzmann, and M. Blumthaler, "All-sky imaging: a simple, versatile system for atmospheric research," *Appl. Opt.* **48**, 1091–1097 (2009).
3. M. S. Ghonia, B. Urquart, C.W. Chow, J.E. Shields, A. Cazorla, and J. Kleissl, "A method for cloud detection and opacity classification based on ground based sky imagery," *Atmos. Meas. Tech.* **5**, 2881–2892 (2012).

News

NIWA UV Workshop

Richard McKenzie (Emeritus Scientist, Workshop Convenor)

NIWA, Lauder, New Zealand

The NIWA-sponsored UV Workshop (<http://www.niwa.co.nz/atmosphere/uv-ozone/uv-science-workshops/2014-uv-workshop>) which was held at the Heritage Hotel, Auckland from 15-17 April was hugely successful. Co-sponsors from New Zealand included the Cancer Society, the Health Promotion Authority, the Dermatological Society, and the Royal Society. Two agencies from Australia also helped to sponsor the event: The Australian National University, and the Queensland Institute of Technology. The diversity of these sponsoring agencies attests to the wide-ranging implications of changes in UV, and its importance in a wide variety of fields. That diversity was also reflected in the diversity of attendees. UV radiation is truly at the crossroads of a wide range of research and health disciplines.

Extended abstracts from most of the presentations are now available on the Workshop web page above. Details of the aims of the workshop, and why the UV situation in New Zealand is so special are summarised in the first article. One of the aims is to improve the dissemination

of UV information. In that regard, several new Apps are available or under development to provide daily UVI forecasts. The detailed information these will provide will be a big step up from what is currently available to the public of New Zealand through the media.

There were approximately 100 registrants at the meeting, which more than for any of the previous 5 UV workshops convened since NIWA's inception. Compared with previous UV Workshops, there was a much stronger international representation, with 20 from Australia, and with representatives from USA, UK, Germany, Switzerland, Japan, Thailand, and Korea. There was also a much stronger emphasis on health impacts, and the delivery of UV information to the public. A highlight was a panel discussion on the question of impacts of UV on vitamin D, and the relationship between vitamin D and health. In total, there were 34 oral presentations, and 12 poster presentations. Abstracts from the previous workshops held in 2002, 2006, and 2010 are also accessible from the above web site.

